ChemistrySelect

Review
doi.org/10.1002/slct.202104290

Chemistry Europe
European Chemical Societies Publishing

www.chemistryselect.org

Medicinal Chemistry & Drug Discovery

Recent Progress in Metal-Incorporated Acyclic Schiff-Base Derivatives: Biological Aspects

Bikash Dev Nath,[a] Md. Monarul Islam,*[a] Md. Rezaul Karim,[a] Shofiur Rahman,[b] Md. Aftab Ali Shaikh,[c, d] Paris E. Georghiou,[b] and Melita Menelaou[e]

Schiff-base derivatives are widely used organic compounds and their metal complexes have been drawing much attention to chemists due to interesting structural features and unique properties. The presence of nitrogen containing imine groups (–C=N–) in Schiff-bases as well as in their metallic complexes and the chelating properties of these compounds are responsible for their many unique biological properties. In this review, we have summarized various acyclic Schiff-base ligands and their different metallic complexes which have been reported in the last one decade. Schiff-bases and their metal complexes have shown a broad range of biological activities, including antifungal, antibacterial, antimalarial, antiproliferative, anti-inflammatory, antiviral, and antipyretic properties. We have reviewed and arranged the reported Schiff-base derivatives according to their diverse biological applications, especially their anti-bacterial and anti-fungal activities, anti-tumor and anti-cancer activities, anti-oxidant activities, anti-inflammatory activities and other therapeutic and medicinal properties. The other component of this work as a review of the molecular structures of various Schiff-bases since their molecular structures play a primary role in the biological properties. The presence of heteroatoms such as nitrogen, sulfur and oxygen with free electron pairs and aromatic rings in the structure of the Schiff-bases play significant roles in determining their properties.

1. Introduction

1.1. Schiff-bases and their Different Derivatives

Schiff-bases, which are named after their discoverer, the German chemist Hugo Schiff,[1,2] are a class of imines formed by the condensation reactions between aldehydes and some ketones, with compounds having primary amino groups such as *e.g.* primary amines, hydroxylamine and hydrazine, etc. Schiff-bases can be formed either intra- or intermolecularly under diverse reaction conditions and in different solvents,[3–7] and have the general formula, $R_1R_2C{=}N{-}R_3$, where R_1, R_2 and R_3 may be an alkyl, aryl or any heteroaryl group (Figure 1). The reactions[1–13] involved in the preparation of a wide variety Schiff-bases require mild reaction conditions and due to their ease of formation, Schiff-bases[1–13] and their derivatives.[14–31] have been widely used in diverse applications.

The various types of Schiff-bases which have come to be known as salens,[19,20] salophens,[21] hydrazones,[22–26] semicarbazones and thiosemicarbazones[27–31] have attracted much attention from researchers since these molecules can form many different derivatives having various application possibilities.[14–31] Schiff-bases can be cyclic[32–34] and non-cyclic.[34] Macrocyclic Schiff-bases[32–34] have found important applications in macrocyclic and supramolecular chemistry, and various heterocyclic Schiff-bases and their derivatives play crucial roles in medicinal chemistry.[35,36] Furthermore, depend-

[a] *Dr. B. D. Nath, Dr. M. M. Islam, M. R. Karim*
Chemical Research Division,
Bangladesh Council of Scientific and Industrial Research (BCSIR) Dhanmondi,
Dhaka-1205, Bangladesh
E-mail: mmipavel@yahoo.com
[b] *Dr. S. Rahman, Dr. P. E. Georghiou*
Department of Chemistry,
Memorial University of Newfoundland,
St. John's, Newfoundland and Labrador,
A1B 3X7, Canada
[c] *Dr. M. A. A. Shaikh*
Bangladesh Council of Scientific and Industrial Research (BCSIR) Dhanmondi,
Dhaka-1205, Bangladesh
[d] *Dr. M. A. A. Shaikh*
Department of Chemistry, University of Dhaka
Dhaka-1000, Bangladesh
[e] *Dr. M. Menelaou*
Cyprus University of Technology
Limassol, 3036, Cyprus

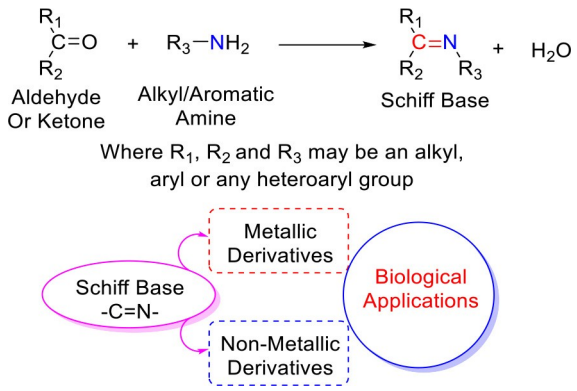

Figure 1. Schematic illustration of the formation of Schiff-bases.

ing on their particular structural features Schiff-bases, both metallic and non-metallic derivatives can be easily synthesized.

1.2. Biological Aspects of Schiff-bases

Schiff-bases possess significant chelating properties and consequently can have potential inherent biological activities. Due

Dr. Bikash Dev Nath received his B.Sc (Hons.) and MS degree in Chemistry from Jahangirnagar University, Bangladesh. He completed his MS thesis in the area of organometallic chemistry under the supervision of Prof. Dr. Shariff Enamul Kabir. He worked as a synthesis engineer (R & D) at Pilarquim (Shanghai) Co., Ltd. in Shanghai, China from 2011 to 2016 where he worked in the development of agrochemical products. He obtained his PhD in 2019 from Okayama University under the supervision of Prof. Dr. Tadashi Ema. He conducted his doctoral research in the area of 'metal complexes and catalysis. His research interests include organic and organometallic synthesis, synthesis of transition metal complexes, catalyst development and study, synthesis of agrochemicals and their biological activities. Since June, 2020, he is working as a Postdoctoral Research Fellow at CRD, BCSIR laboratories Dhaka in Dr. Md. Monarul Islam's research group.

Dr. Md. Monarul Islam obtained both B.Sc (Hons.) and MS degrees in Chemistry from the University of Dhaka, Bangladesh. He was appointed as a Scientific Officer in the Chemical Research Division (CRD), BCSIR Laboratories, Dhaka in 2009 and in 2017 he was promoted to Senior Scientific Officer. His doctoral work was conducted in the group of Prof. Takehiko Yamato at Saga University, Japan (2015). His current research focuses on the synthesis and development of new functional organic molecules and macrocycles for organic optoelectronics and biological applications. He is interested in initiating science leadership programs for young scientists in Bangladesh to improve their research environments and motivation. He is a founding member of National Young Academy of Bangladesh (NYAB). He also worked as a Postdoctoral Research Associate (Talented Young Scientists Program Fellow) at Guangdong University of Technology, Guangzhou, P R China from October 2018 to September 2019 in Dr. Xing Feng's research group.

Md. Rezaul Karim is currently working as a Research Chemist from 2019 at BCSIR Laboratories, Dhaka. Bangladesh Council of Scientific and Industrial Research (BCSIR). Now he is doing research on polymeric chemistry for the development of new advanced polymeric soft materials like hydrogel, biodegradable packaging material. He received his M.Sc. from Bangladesh University of Engineering and Technology (BUET), Bangladesh in the field of polymeric smart materials. He has attended 6 international and national conference and got best presentation award in 5th Conference of Bangladesh Crystallographic Association, Bangladesh.

Dr. Shofiur Rahman is currently a Research Associate at Memorial University of Newfoundland in St. John's, NL, Canada. He received his Ph.D. degree in Organic Chemistry, Energy and Material Science from Saga University, Japan in 2007. Before joining Memorial University, he worked at the National Institute for Nanotechnology (NINT), University of Alberta in Edmonton, Canada. Before coming to Canada, he was a Faculty member at Khulna University of Engineering & Technology, Bangladesh. He obtained both B.Sc (Hons.) and MSc degrees in Chemistry from the University of Rajshahi, Bangladesh. He obtained his Master of Philosophy (M.Phil.) degree in Chemistry from Bangladesh University of Engineering & Technology (BUET), Dhaka, Bangladesh. Before coming to Canada, he was a Faculty member at Khulna University of Engineering & Technology, Bangladesh. He has published 60 research papers with his colleagues in peer-reviewed international journals. His research interests are in the areas of supramolecular chemistry and synthesis of calixarenes and cyclophanes, computational chemistry, chemical sensors, bio-oils and ionic liquids.

Dr. Md. Aftab Ali Shaikh is a Professor, Department of Chemistry, University of Dhaka, Bangladesh. Dr. Shaikh obtained his both B.Sc (Hons.) and MSc degree in Chemistry from University of Dhaka. He completed his doctoral degree from Liebniz University of Hannover, Germany in Material Science under the supervision of Professor Dr. J. Christian Buhl. He joined as a Lecturer in the Department of Chemistry in 2000 and promoted to Professor in 2013. Dr. Shaikh was a Postdoctoral Research Fellow in University of Bonn in Professor Dr. Robert Glaum's group. In his professional career, he holds many important positions in University of Dhaka, such as Assistant Proctor, Senate & Syndicate member, Director of Institute of Leather Engineering and Technology. He was a general secretary of Bangladesh Chemical Society (2018-2019). Currently, he is the general secretary of Bangladesh Crystallographic Association (BCA). He is working as a Chairman of Bangladesh Council of Scientific and Industrial Research (BCSIR) since August, 2020.

Professor Paris E. Georghiou is an Honorary Research Professor of Chemistry at Memorial University of Newfoundland, St. John's, Newfoundland and Labrador, Canada where he has been on the Faculty since 1975. He earned his BSc (Hons) from the University of the Witwatersrand, Johannesburg, South Africa and his PhD with Professor George Just, in Organic Chemistry from McGill University, Montreal Quebec, Canada in 1971. After teaching at Dawson College CEGEP in Montreal he took up a Postdoctoral Fellowship with Professor Satoru Masamune at the University of Alberta in Edmonton, Alberta, Canada from 1973–1975. He has over 120 paper in peer-reviewed publications and journals and in a wide range of chemistry and with many international collaborators as a result of research work that he and his graduate students and Postdoctoral associates and colleagues have conducted. His research interests are in Organic Synthesis, Structural, Medicinal, Supramolecular, Enironmental, Computational and Analytical Chemistry. In particular, he has published extensively in the general area of macrocyclic compounds, including calixarenes, calixnapthalenes and cyclophanes, the latter in on-going collaboration with Professor T. Yamato, Dr. M. M. Islam, Rahman and Menelaou.

Dr. Melita Menelaou is a Chemical Engineer, PhD educated, with experience in multidisciplinary research in the broad field of Materials Chemistry and Materials Engineering. During her career, she enhanced her knowledge and expertise as a member of respected research groups in Japan – Advanced Institute of Materials Research (WPI-AIMR), Tohoku University, Czechia – Central European Institute of Technology-Brno University of Technology (CEITEC-BUT), Spain - University of Barcelona, and Greece – School of Chemical Engineering, and School of Chemistry, Aristotle University of Thessaloniki (AUTh). Her research interests are in Nanoscience, Molecular Chemistry, and Spectroscopic and Magnetic Characterization of Materials, among others.

to their structural flexibility, they can be synthetically modified and fine-tuned for specific biological applications and many metallic[3,15,17,18,37–39] and non-metallic[15,40–44] derivatives of Schiff-bases are being researched extensively to develop new compounds with desired biological properties. The imine or azomethine group in structure-activity relationship (SAR) studies of Schiff-bases have shown the considerable chemical and biological importance for the lone pair of electrons in the sp^2- hybridized orbital of nitrogen atom of the –C=N– group.[45,46] Schiff-bases may interfere in normal cell processes by the formation of a hydrogen bond between the nitrogen of the –C=N– group and the active centers of cell constituents.[47–49]

1.3. Metal Complexes of Schiff-base derivatives and their Biological Properties

Schiff-bases can coordinate with metal centers through the imine groups (–C=N–) and as a result, the Schiff-base double bond can either be stabilized or labilized thermodynamically by the metal ions.[50] The biological properties of the metallic derivatives of acyclic Schiff-base ligands arise from the increased lipophilicity of the metal complexes resulting from the chelation of the ligands with the metal elements, which decreases the polarity of the coordinated metal ions by partial sharing of their positive charges with the donor groups.[51] As a consequence of the improved lipophilic character due to the delocalization of π-electrons over the whole chelate moeity, these metal complexes can interfere with the normal cell processes by interacting with the cell constituents e.g. by effectively permeating the lipid layer of the microorganism. This can also be explained by Overtone's concept of cell permeability[51b] and Tweedy's chelation theory.[51c]

The enhanced biological activities[52–54] of the metallic derivatives of Schiff-bases stem from the chelating Schiff-base ligands containing N donor atom which can be bonded to the metal ions in a variety of ways, give rise to their advanced anti-bacterial,[55] anti-viral,[56] anti-malarial,[57] anti-fungal,[58] anti-tubercular,[59] anti-tumor,[60] anti-angiogenic,[61] anti-cancer,[61,62] anti-inflammatory,[63] anti-oxidant[64] and other therapeutic and medicinal activities. Most recently, medicinal chemists and biologists have shown much intererest in Schiff-bases and their transition metal complexes.

1.4. Scope of this Review

Numerous Schiff-bases and their derivatives have been reported to possess promising biological properties and several review articles have been published in the past few years.[37–44] Recently, review articles regarding the biological applications of macrocyclic Schiff-base ligands and their metal complexes have been published.[32,34] However, no comprehensive review has been published recently on the biological properties of metallic derivatives of acyclic Schiff-base ligands. Herein we provide a broad overview of recent advances of metallic derivatives of acyclic Schiff-base ligands and their biological applications which have appeared during the last decade. The aim of this review is to present the recent literature insights into the structure-activity relationships of various Schiff bases and their metallic derivatives and which are summarized at the conclusion.

2. Recent Development of Acyclic Metal Complexes of Schiff-base Derivatives and their Biological Applications

Many Schiff-base metal complexes synthesized from acyclic Schiff-base ligands which have shown remarkable anti-bacterial biological properties have been reported. These were targeted to determine the behavior of the metal complexes in which chelation plays a significant role. However, several other important factors such as the geometry of the complexes, bond lengths between the metal and the ligand, dipole moment, coordinating sites, redox potential of metal ion, solubility, steric, pharmacokinetics, concentration and hydrophobicity can also influence substantially. Some of the recently developed metal complexes as well as their diversified biological applications are reviewed below:

2.1. Metal Complexes Exhibiting Anti-bacterial and Anti-fungal Activities

The antibacterial and antifungal activities of Schiff base metal complexes have been found to be significantly different to those of their parent Schiff-base ligands as shown by the following examples. Sengupta and co-workers synthesized the neodymium(III) complexes $[Nd(L^1)Cl(H_2O)_3]$ **1**, $[Nd(L^2)Cl(H_2O)_3]$ **2** and $[Nd(L^3)Cl(H_2O)_3]$ **3** from Schiff-bases **L1**–**L3** (Figure 2) which showed good antibacterial activities with respective inhibition zones (IZ) of 86.5, 79.5 and 70.1 % at 100 μg mL^{-1} against Gram-positive bacteria (*B. subtilis*). A similar trend was observed for their antifungal activities showing inhibition zones of 88.3, 80.2 and 70.2 %, respectively against *A. niger*.[65] The metal complexes were found to be more active than the free Schiff-base ligands.

Mahmoud and co-workers reported Co^{II}, Ni^{II} and Zn^{II} complexes **4–6** of benzoic acid containing Schiff-base ligand **L4** (Figure 3). The Co^{II} and Ni^{II} complexes **4** and **5** showed clear anti-bacterial activities against two Gram-positive bacteria (*B. subtilis* and *S. aureus*) and two Gram-negative bacteria (*E. coli* and *N. gonorrhoeae*).[66] They also showed anti-fungal activities

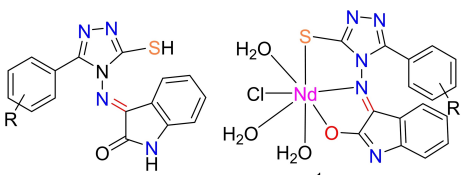

Figure 2. Structures of Schiff-base ligands (**L1**–**L3**) and the corresponding Nd^{III} complexes, **1**–**3** synthesized from these ligands.[65]

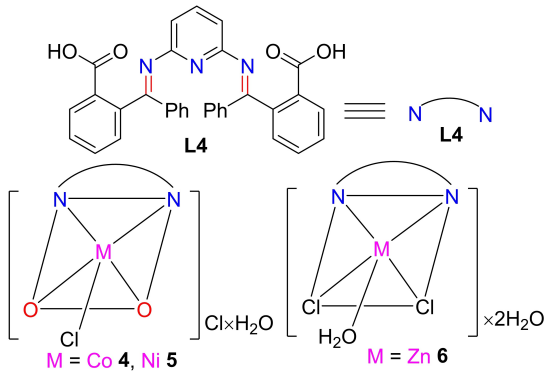

Figure 3. Structures of Schiff-base ligand, **L4** and its Co^{II}, Ni^{II} and Zn^{II} complexes **4**–**6**.[66]

against the fungus strain *C. albicans*. The Zn^{II} complex **6** showed good anti-bacterial activities against *B. subtilis*, *E. coli* and *N. gonorrhoeae*.[66] Ebrahimipour's group studied the anti-bacterial and anti-fungal activities of the Schiff-base ligands H_2L^1 (**L5**) and H_2L^2 (**L6**) and their corresponding uranyl(VI) complexes $[UO_2(L^1)(DMSO)]$ **7** and $[UO_2(L^2)(MeOH)]$ **8** (Figure 4) changed here.[67] The anti-bacterial and anti-fungal activities of the complexes were tested by evaluating the inhibition zone (IZ), minimal inhibitory concentration (MIC) and minimal bactericidal concentration (MBC) values. Complexes **7** and **8** can clearly seen to be derived from the enol-forms of the respective keto-enol tautomers of the Schiff base ligands **L5** and **L6**.

Both uranyl(VI) complexes **7** and **8** exhibited anti-bacterial activities only against Gram-positive bacteria, showing respectively, IZ values of 8.0 and 21 mm against *S. aureus* PTCC 1112 and 9.0 and 33 mm against *M. luteus* PTCC 1110. Furthermore, both complexes showed no activity against Gram-negative bacteria (*E. coli*) whereas the standard anti-bacterial agent ciprofloxacine displayed no selectivity against either Gram-positive or Gram-negative species. The U^{VI} complexes also showed anti-fungal activities with respective IZ values of 8.5 mm and 19 mm for **7** and **8** against *C. albicans* PTCC 5027, respectively. The anti-microbial activities of Schiff-base ligand H_2L^1 (**L5**) were higher than those of H_2L^2 (**L6**), whereas **8** showed greater activities than **7**. The Schiff-base ligand H_2L^2 (**L6**) and both U^{VI} complexes **7** and **8** showed MIC and MBC values in the range of 30 to 0.118 mg mL^{-1} whereas these values for H_2L^1 (**L5**) were in the range of 10 mg mL^{-1} to 39 μg mL^{-1}. The Schiff-base ligand, H_2L **L7** and their dioxomolybde-num(VI) complexes $[MoO_2L(THF)]$ **9**, $[MoO_2L(1\text{-methimz})]$ **10**, $[MoO_2L(1\text{-allylimz})]$ **11** and $[MoO_2L(\gamma\text{-pic})]$ **12** (Figure 5) developed by Pramanik, Chakrabarti and co-workers, showed moderate anti-bacterial activities (MIC values in the range, 1.0–10.0 μg per disc (determined by the disc diffusion method)) against two Gram-positive bacteria (*B. cereus*, *B. subtilis*), three Gram-negative (*P. vulgaris*, *E. coli*, *P. aeruginosa*) and one yeast (fungus) (*C. albicans*).[68]

Singh's group pointed out that Gram-negative bacteria possess relatively more complex cell walls compared to those of Gram-positive ones,[69] and suggested that this could be a reason why the metallic derivatives of Schiff-bases can diffuse

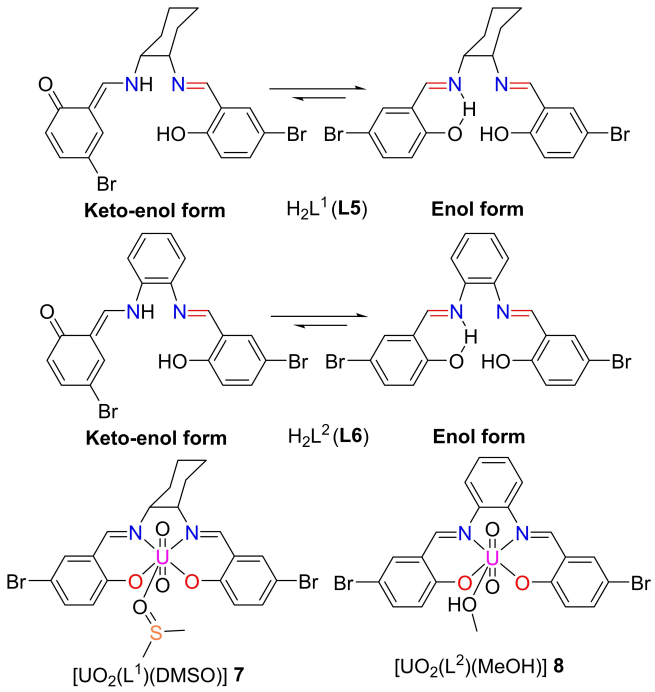

Figure 4. Structures of Schiff-base ligands, **L5**–**L6** and uranyl(VI) complexes, **7**–**8**.[67]

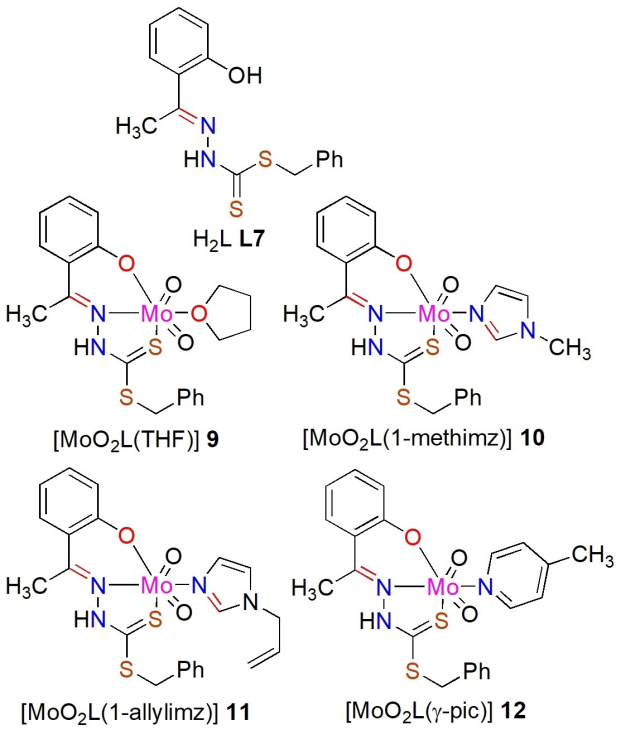

Figure 5. Structures of dioxomolybdenum (VI) complexes $[MoO_2L(THF)]$ **9**, $[MoO_2L(1\text{-methimz})]$ **10**, $[MoO_2L(1\text{-allylimz})]$ **11** and $[MoO_2L(\gamma\text{-pic})]$ **12**.[68]

through the Gram-negative bacterial cells more efficiently than the Gram-positive ones. Several bifunctional tridentate Schiff-bases and their triphenyltin(IV) and trimethyltin(IV) derivatives (structures not shown) were found to be more toxic against the Gram-positive *B. subtilis* than against the Gram-negative *E. coli*.[69] The authors reported that the electron-withdrawing nature of the phenyl groups present in the ligand enhanced the anti-bacterial activity of triphenyltin(IV) derivatives as they effected greater electron deficiency in the central tin atom, in comparison with the trimethyltin(IV) derivatives where the electron-donating methyl groups enhanced the electron density at the central metal atom.[69]

The anti-bacterial activities of several coordination compounds of metal(II) ions of the bis-Schiff-base ligand H_2 L, L8 (Figure 6) have been reported.[70] Among the complexes, the Co^{II} complex **13** exhibited the highest anti-bacterial activities against several organisms, both Gram-positive (*B. subtilis* and *S. pyogones*) and Gram-negative (*P. vulgaris* and *E. coli*). The highest diameter of IZ; namely, 45 and 37 mm were found for *B. subtilis* and *S. pyogones*, respectively, with corresponding MIC_{50} values of >25 and >50 mg mL^{-1} whereas for the Gram-negative bacteria *P. vulgaris* and *E. coli*, the respective IZs were 32 mm (MIC_{50} value of >50 mg mL^{-1}) and 30 mm (MIC_{50} value of >50 mg mL^{-1}), respectively. The anti-bacterial activity of Co^{II} complex was higher than that of the parent ligand, H_2L **L8**.

Remarkable anti-fungal activities for Ni-complexes, $Ni_2(L^1)_2$ **14** and $Ni(H_2L^2)$ **15** (Figure 7) against *A. niger* (MTCC-281), *C. candidum* (MTCC-3993), *C. albicans* (MTCC-227), and *C. tropicalis* (MTCC-230) were reported by Singh's group. The MIC values for the two complexes **14** and **15** against these four strains were respectively as follows: (100 and 150) μg mL^{-1}, (201 and 203) μg mL^{-1}, (150 and 189) μg mL^{-1} and (110 and 103) μg mL^{-1}. These values were higher than those obtained for the Schiff-base ligands, H_2L^1 **L9** and H_4L^2 **L10**.[71]

The authors also reported higher anti-bacterial activity for the metal complexes than those of the ligands alone. Both $Ni_2(L^1)_2$ and $Ni(H_2L^2)$ complexes **14** and **15** were the most effective against *S. aureus* (MTCC-740) with corresponding MIC values of 14 μg mL^{-1} and 18 μg mL^{-1}, respectively, and against *E. coli* (MTCC-119) with corresponding MIC values of 73 μg mL^{-1} and 77 μg mL^{-1}. On the other hand, the MIC values for the Schiff-base ligands, H_2L^1 **L9** and H_4L^2 **L10** against these two bacteria are (80 and 83) μg mL^{-1} and (100 and 95) μg mL^{-1}, respectively. This behavior of the complexes might be attributed to their abilities to cause damage to the biomolecules within the cell or the cell surface due to the high redox potential, high toxicity at the cell surface and/or structural specificity.Two metal complexes of the phenoxymethylpenicillin-based Schiff-base ligand HL **L11**, namely, $[FeL(OAc)(H_2O)_2]$ **16** and $[NiL(OAc)(H_2O)_2]$ **17** (Figure 8) showed higher anti-bacterial activities than the ligand HL **L11** itself, against *S. viridans*, *E. sp*, *S. aureus*, *E. faecalis* and *Methicillin-resistant S. aureus* (MRSA).[72] The metal complex $[FeL(OAc)(H_2O)_2]$ **16** against these five strains showed IZs of 20 mm, 30 mm, 25 mm, 22 mm and 15 mm; whereas the corresponding values for $[NiL(OAc)(H_2O)_2]$ **17** against the five bacteria were observed as 10, 40, 36, 27, and 18 mm, respectively. The IZs for the Schiff-base ligand HL **L11** were respectively found to be 15, 24, 16, and 17 mm, as well as resistant, respectively.[72] Complex, $[FeL(OAc)(H_2O)_2]$ **16** proved to be the most effective against MRSA (MIC value: 0.042 μmol mL^{-1}) while $[NiL(OAc)(H_2O)_2]$ **17** showed the highest activity against both *E. sp and S. aureus* (MIC values of 0.042 μmol mL^{-1}).[72]

Three metal(II) complexes; namely, $[Ni^{II}L(H_2O)Cl]_x4H_2O$ **18**, $[Cu^{II}L(H_2O)Cl]_x3H_2O$ **19**, and $[Zn^{II}L(H_2O)Cl]_x5H_2O$ **20** (where, L = 2-furan-2-ylmethyleneamino-phenyl-iminomethyl phenol) were synthesized from the Schiff-base ligand, HL **L12** (Figure 9) and were studied for both the anti-bacterial and anti-fungal activities. The microorganisms which were tested were: two Gram-positive bacteria species, namely *S. pneumonia* and *B. subtilis*, and two Gram-negative bacteria, *S. typhi* and *E. coli*, in addition to four fungi species, *A. fumigatus*, *S. racemosum*, *G.*

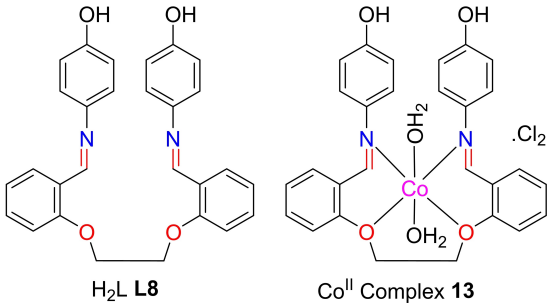

Figure 6. Structures of bis-Schiff-base ligand **L8** and Co^{II} complex **13**.[70]

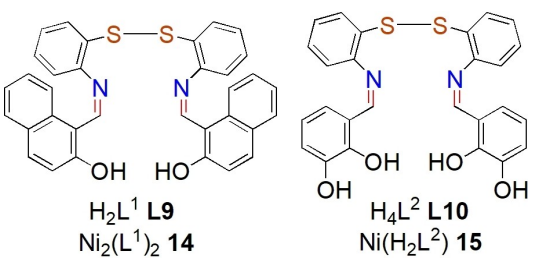

Figure 7. Structures of chitosan Schiff-base ligands **L9-L10** and the Ni^{II} complexes **14–15**.[71]

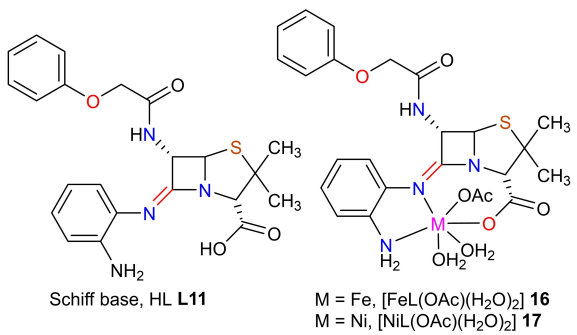

Figure 8. Structures of phenoxymethylpenicillin-derived Schiff-base ligand, HL **L11** and it's metallic derivatives.[72]

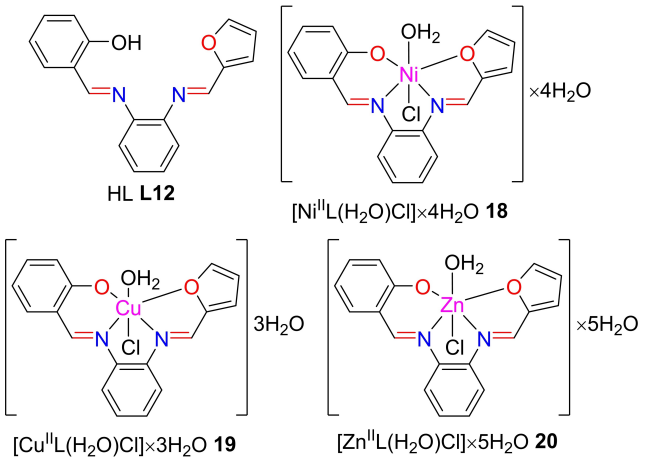

Figure 9. Structures of Schiff-base ligand, **L12** and Ni^{II}, Cu^{II} and Zn^{II} complexes, **18–20**.[73]

candidum, and *C. tropicalis*.[73] Although the ligand **L12** alone showed no activity against all of these sensitive organisms, inhibitory activity was enhanced upon complexation especially in the case of Ni^{II}, Cu^{II}, and Zn^{II} complexes **18–20**, even though it was less than the standard. All three metal complexes were tested against *S. pneumonia, B. subtilis* and *E. coli*. The Cu^{II} complex **19** showed highest IZ against all three pathogens (16.4, 18.4, and 21.2 mm). The authors also tested the anti-fungal activities against two pathogens; namely, *A. fumigatus*, and *G. candidum* and, the Cu^{II} complex **19** complex similarly showed the highest activity among the three synthesized complexes.

Tripathi's group studied the anti-bacterial and anti-fungal activities of Pr^{III} complexes $[Pr(C_{15}H_{12}N_2OH)(6H_2O)Cl_2]_x1.5H_2O$ **21**, and $[Pr(C_5H_{10}NS_2)(C_{15}H_{12}N_2O{\cdot}OCH_3)(3H_2O)Cl]$ **22** (Figure 10).[74] The anti-bacterial activity of complex **22** was found to be enhanced compared to the free ligand, exhibiting the maximum inhibition of bacterial growth against *P. aeruginosa* (25 mm) and *E. coli* (18.0 mm). The maximum inhibition of fungal growth however was observed for the case of complex **21** against *C. albicans* which was higher than that of the ligand. Upon complexation, the biological activity of the complexes increased. Prabhakaran's group also reported similar enhancement in anti-bacterial and anti-fungal activities when cyclometallated Ru^{II} complex **23** was prepared from the complexation of the Schiff-base ligand, 3-acetyl-7-meth-oxycoumarin-4 *N*-substituted thiosemicarbazone with $[RuHClCO(PPh_3)_3]$ as the metal precursor.[75]

Devi and co-workers observed that the electron-releasing effects of chloro and bromo groups on the benzene ring influenced the anti-bacterial activities of the Zn^{II} complexes such as $Zn(L^1)_2{\cdot}2H_2O$ **24**, $Zn(L^2)_2{\cdot}2H_2O$ **25**, $Zn(L^3)_2{\cdot}2H_2O$ **26** and $Zn(L^4)_2{\cdot}2H_2O$ **27** (Figure 11) against the Gram-positive bacterial strains *S. aureus* (with respective MIC values of 0.0380, 0.0286, 0.0179 and 0.0319 $\mu M\,mL^{-1}$); *S. gordonii* (with respective MIC values of 0.0380, 0.0286, 0.0359 and 0.0319 $\mu M\,mL^{-1}$); and the Gram-negative bacterial strains *E. coli* (with respective MIC values of 0.0190, 0.0287, 0.0359 and 0.0160 $\mu M\,mL^{-1}$), and *P. aeruginosa* (with respective MIC values of 0.0190, 0.0143, 0.0359 and 0.0160 $\mu M\,mL^{-1}$).[76]

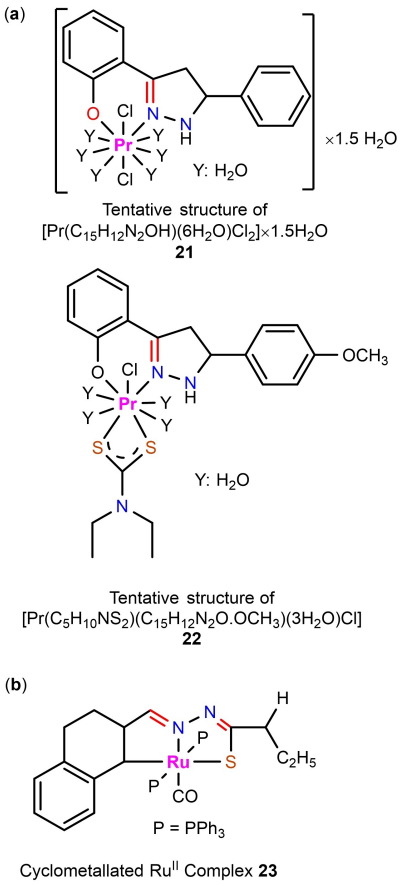

Figure 10. Structures of (a) Pr^{III} complexes $Pr(C_{15}H_{12}N_2OH)(6H_2O)\,Cl_2]_x1.5H_2O$ **21**, $[Pr(C_5H_{10}NS_2)(C_{15}H_{12}N_2O{\cdot}OCH_3)(3H_2O)Cl]$ **22**[74] and (b) Cyclo-metallated Ru^{II} complex **23**.[75]

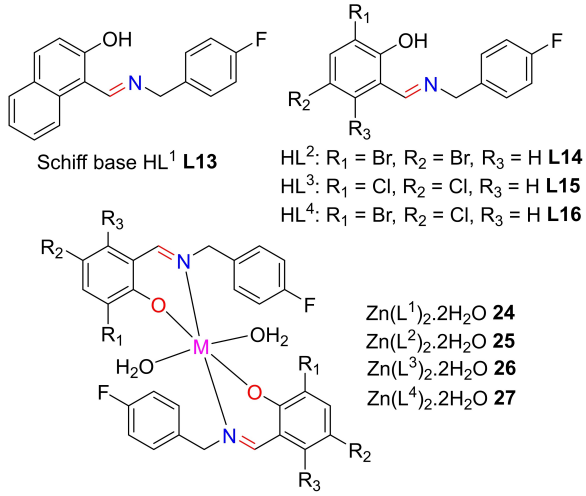

Figure 11. Structures of Schiff-base ligands **L13–L15** and Zn^{II} complexes **24–27**.[76]

The compounds also exhibited remarkable anti-fungal activities against *C. albicans* (respective MIC values of 0.0190, 0.0009, 0.0006 and 0.0010 μM mL^{-1}) and *A. niger* (respective MIC values of 0.0190, 0.0140, 0.0180 and 0.0080 μM mL^{-1}). The aforementioned complexes were more active than their corresponding Schiff-base ligands.

The Pawar group also reported Zn^{II} complexes in the form of $Zn(HL^1)_2$ **28** and $Zn(HL^3)_2$ **29** which were synthesized from the Schiff-base ligands HL^1 **L17** and HL^2 **L18**. Complex $Zn(HL^2)_2$ **29** showed the highest anti-bacterial activities against *S. aureus*, *B. subtilis*, *E. coli* and *S. typhi* with corresponding MIC values of 3.90, 7.81, 62.5 and 125 μM mL^{-1}, respectively (Figure 12).[77] Although $Zn(HL^1)_2$ **28** showed similar MIC values against *B. subtilis*, *E. coli* and *S. typhi*, the anti-bacterial activity of this complex was lower than that of $Zn(HL^2)_2$ **29** against *S. aureus*.

Misra's group synthesized Mn^{II} and Co^{II} complexes from the Schiff-base ligand 2-acetyl-5-methylsemicarbazone.[78] Zoubi, Ko and co-workers reported remarkable anti-bacterial and anti-fungal activities of Ni^{II}, Zn^{II}, Cd^{II}, Hg^{II}, Pt^{II} and Pd^{II} complexes derived from the Schiff-base ligand 4-[(2,4-dimethoxy-benzylidene)-amino]-1,5-dimethyl-2-phenyl-1,2-dihydro-pyrazol-3-one.[79] Peewasan, Powell and co-workers prepared a pair of polynuclear chiral Cu^{II}-cluster complexes which in their enantiomeric pure forms showed good anti-bacterial activities against Gram-positive bacteria.[80] Quite remarkable anti-microbial activities of three metal complexes $[Co(HL)(H_2O)Cl_2]_xH_2O$ **30**, $[Ni(HL)(H_2O)Cl_2]$ **31** and $[Zn(HL)(H_2O)Cl_2]_xH_2O$ **32** against the Gram-positive (*S. aureus* and *B. Subtilis)*, Gram-negative (*Salmonella SP.*, *E. coli* and *P. aeruginosa*, as well as fungi (*A. fumigatus* and *C. albicans*) were reported (Figure 13).[81] All of the complexes exhibited higher anti-bacterial and ant-fungal activities than those of the Schiff-base ligand HL **L19** (Figure 13b). $[Co(HL)(H_2O)Cl_2]_xH_2O$ **30** showed the highest anti-bacterial activities against the Gram-negative bacteria *E. coli* (IZ: 17 mm) and *P. aeruginosa* (IZ: 18 mm). $[Ni(HL)(H_2O)Cl_2]$ **31** also displayed higher anti-bacterial activities against Gram-negative bacteria *S. SP.* (IZ: 17 mm), *E. coli* (IZ: 18 mm) and *P. aeruginosa* (IZ: 19 mm). On the other hand, $[Zn(HL)(H_2O)Cl_2]_xH_2O$ **32** showed the highest ant-bacterial activities against Gram-positive bacteria *B. subtilis* (IZ: 17 mm) and Gram-negative bacteria *S. SP.* (IZ: 18 mm). Both $[Ni(HL)(H_2O)Cl_2]$ **31** and $[Zn(HL)(H_2O)Cl_2]_xH_2O$ **32** complexes showed more activity against the fungal strain, *C. albicans* (IZ: 16 and 17 mm, respectively).

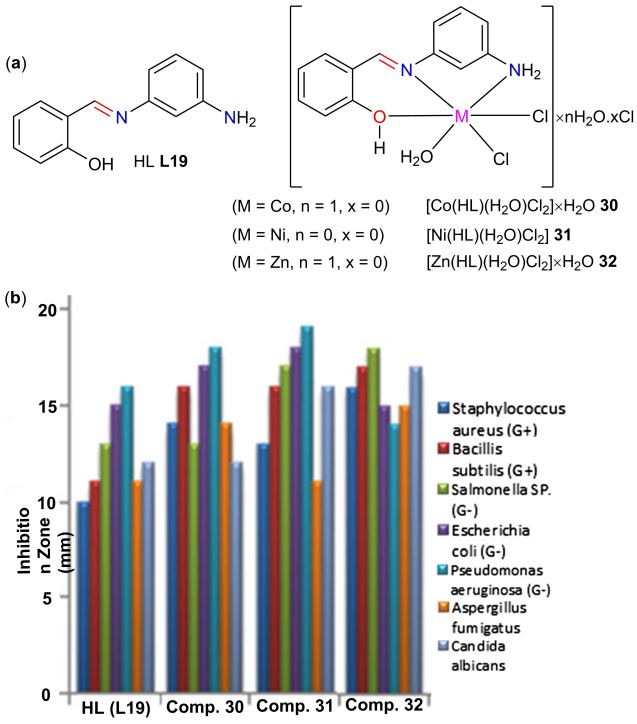

Figure 13. (a) Structures of Schiff-base ligand **L19** and M^{II} complexes **30–32**. (b) Anti-microbial activities of ligand **L19** and M^{II} complexes **30–32** (Reproduced from Ref. [81]. Copyright (2019) Wiley-VCH.).[81]

Sithique and co-workers reported Zn^{II}-centered hydrazide-based *O*-carboxymethyl chitosan Schiff-base metal complexes, **33–34** exhibiting enhanced anti-bacterial and anti-fungal activities (Figure 14).[82] The complexes exhibited a maximum growth inhibition zone of ~40 mm against bacterial strains (such as *E. coli* and *S. aureus*). The complexes showed highest anti-fungal activities against *C. albicans.*

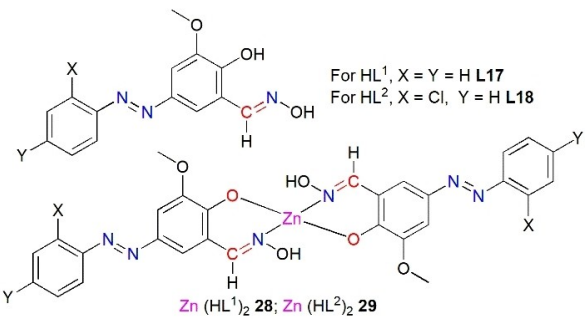

Figure 12. Structures of Schiff-base ligands **L17-L18** and Zn^{II} complexes **28–29**.[77]

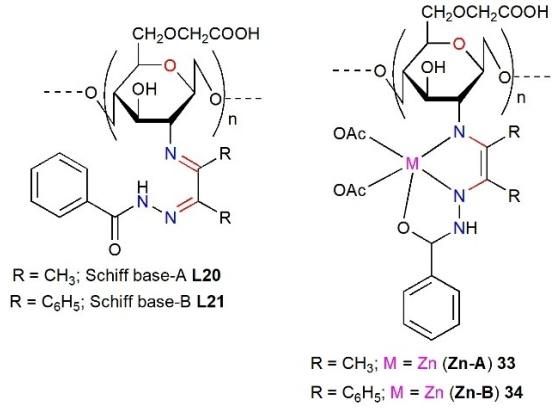

Figure 14. Structures of chitosan Schiff-base ligands **L20–L21** and their Zn complexes **33–34**.[82]

Using a bidentate N_2O_2 Schiff-base ligand, (*E*)-2-bromo-4-chloro-6-[(2,6-dimethylphenylimino) methyl]phenol, HL **L22**, a mononuclear Cu^{II} complex **35** was synthesized by Guo and co-workers. Complex **35** showed high anti-bacterial activities against *S. aureus*, *P. aeruginosa*, and *E. coli* (Figure 15).[83] Complex **35** showed the highest anti-bacterial activity against *E. coli* (MIC value of 1.25 mmol L^{-1}) which was higher than of the ligand (HL) (MIC value of 5 mmol L^{-1}).

The complex also showed much higher anti-bacterial activity against *E. coli* than that of the reference drug Penicillin (MIC value of 10 mmol L^{-1}).[83]

Adam and co-workers synthesized several ONO-Pincer Schiff-base salicylidene (HSaln ligand **L23**) complexes with Mn^{2+}, MoO_2^{2+} and UO_2^{2+} ions (MSaln complexes = MnSaln **36**, MoO_2Saln **37**, and UO_2Saln **38**, respectively) (Figure 16).[84] The MIC values of the HSaln ligand **L23** and its MSaln complexes, **36–38** against the Gram-positive bacterial strain (*S. aureus*), Gram-negative bacterial strains (*S. marcescens*, *E. coli*) and the fungal strains (*C. albicans, A. flavus* and *T. rubrum*) confirmed higher activities of the metal complexes compared to those of the HSaln ligand (**L23**).

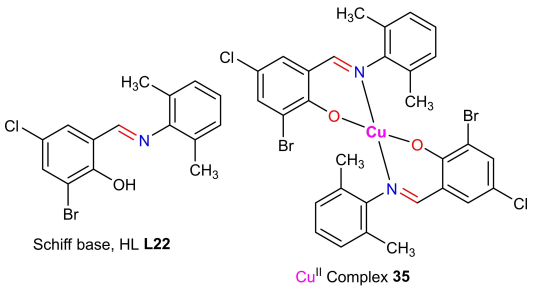

Figure 15. Structures of Schiff-base ligand **L22** and its Cu^{II} complex **35**.[83]

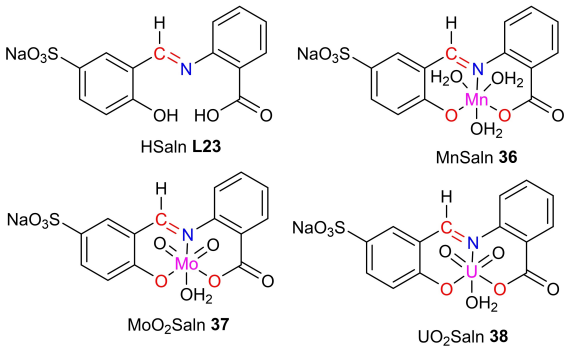

Figure 16. Structures of HSaln ligand, **L23** and MSaln complexes, **36–38**.[84]

The increased anti-microbial potential of MSaln complexes relative to the HSaln ligand (Tables 1 and 2) was attributed to the addition of the metal complexes to the Schiff-base nitrogen atoms (–CH=N–) in which the strongly coordination capability of the central metal ion (M^{2+}) due to its high positive charge, played a significant role in improving the antimicrobial action of the HSaln ligand. Additionally, the lipophilic character of the π-electron delocalized rings over the antimicrobial reagents could have also enhanced their antimicrobial abilities. The *p*-sodium sulfonate groups bonded to one of the phenyl rings rings contributed to the high solubility of the complexes, which in addition to their conductivity, could also account for their valuable antimicrobial action. The low lipid solubility of metal complexes across the microbial walls was found to result in the lower activity of complexes as compared to others.[85]

UO_2Saln **38** and MnSaln **36** complexes were found to exhibit the highest antimicrobial potential (Tables 1 and 2). For both antimicrobial results an additional possible factor could also be the ability of the uranium in the UO_2Saln complex to increase its coordination number as a 4f element and in the case of the MnSaln complex the presence of the higher number of the labile coordinated solvent molecules.

Treatment of multidrug-resistant fungal infections is challenging and the development of new chemotherapeutic agents for this purpose is an important research area to augment the current treatment options. With that objective, Dar *et al.* reported the mixed ligand complexes [Cu(phen)LClH_2O] **39**, [Co(phen)LClH_2O] **40**, [Ni(phen)LClH_2O] **41**, and [Zn-(phen)LClH_2O] **42** (phen = phenanthroline) formed with the Schiff-base ligand, **L24** (Figure 17).[86]

All complexes showed varying levels of anti-fungal activities against several *C. albicans* isolates (including FLC susceptible and resistant *C. albica*ns isolates). From the MIC values, the order of anti-fungal potency of the tested complexes was found to be **39** > **40** > **41** ≥ **42** > **L24**. The MIC values for **41** were found to range from 1–0.25 μg mL^{-1} while as for the **L24** these values ranged from 125–500 μg mL^{-1}. The marked enhancement of anti-fungal activities was associated with the structural changes from the ligand to its metal complexes.

Tavman and co-workers synthesized the Schiff-base ligand H_3L (**L25**) and its Zn^{II} complex, $[Zn(H_2L)Cl]_x4H_2O$ **43** (Fig-

Table 1. Anti-bacterial activities of HSaln ligand **L23** and their different metal complexes (**36–38**) against three bacterial strains. (data taken from Ref. [84])

Compounds (20 μg mL^{-1})	Inhibiton Zone (mm) *S. aureus (+ve)*	*E. coli (-ve)*	*S. marcescens (-ve)*
HSaln ligand (**L23**)	14 ± 0.24	8 ± 0.15	10 ± 0.33
MnSaln (**36**)	42 ± 0.19	34 ± 0.27	36 ± 0.24
MoO_2Saln (**37**)	38 ± 0.17	32 ± 0.19	33 ± 0.12
UO_2Saln (**38**)	44 ± 0.25	35 ± 0.19	38 ± 0.27
Gentamycin	46 ± 0.11	37 ± 0.72	40 ± 0.33

Table 2. Anti-fungal activities of HSaln ligand **L23** and their different metal complexes (**36–38**) against three fungal strains. (data taken from Ref. [84])

Compounds (10 μg mL^{-1})	Inhibiton Zone (mm) *C. albicans*	*A. flavus*	*T. rubrum*
HSaln ligand **L23**	7 ± 0.16	8 ± 0.34	11 ± 0.07
MnSaln **36**	33 ± 0.27	22 ± 0.22	28 ± 0.13
MoO_2Saln **37**	32 ± 0.12	21 ± 0.09	27 ± 0.12
UO_2Saln **38**	36 ± 0.17	24 ± 0.21	30 ± 0.23
Fluconazole	37 ± 0.62	25 ± 0.90	31 ± 0.88

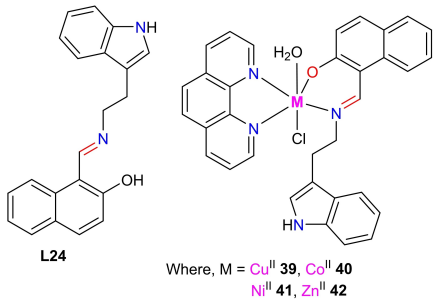

Figure 17. Structures of ligand, **L24** and metal(II) complexes, **39–42**.[86]

ure 18).[87] Complex **43** showed much lower MIC values (superior antifungal activity) on *C. Albicans*, *C. Tropicalis* (< 4.87 μg mL^{-1} for both) and *C. Parapsilosis* (9.75 μg mL^{-1}) compared to those obtained for the Schiff-base ligand H_3L **L25** itself (19.5, 39 and 78 μg mL^{-1} for *C. parapsilosis*, *C. tropicalis* and *C. albicans*, respectively). Complex **43** was also more effective against *S. epidermidis* than the H_3L (**L25**).

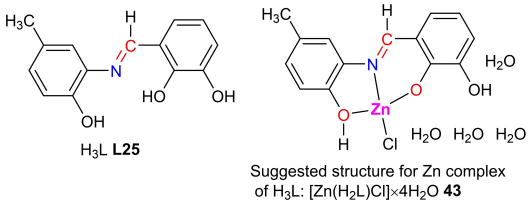

Figure 18. Structures of ligand H_3L **L25** and its Zn^{II} complex **43**.[87]

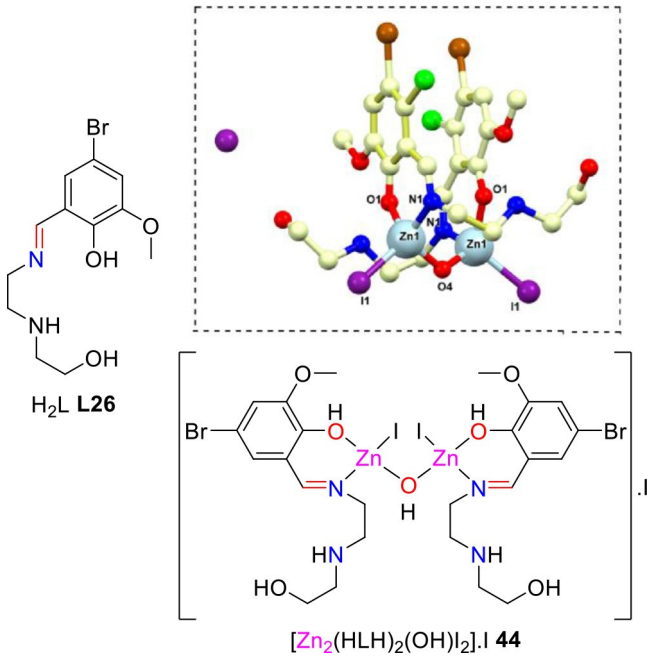

Figure 19. Structures of ligand H_2L **L26** and its Zn^{II} complex **44** (Reproduced from Ref. [88]. Copyright (2020) ACS.).

Das and co-workers obtained the dinuclear Zn^{II} complex, $[Zn_2(HLH)_2(OH)I_2]\cdot I$ **44** from the Schiff-base ligand H_2L **L26** which showed very high anti-bacterial activity against both Gram-positive (*L. monocytogenes*, MIC value: 158.8 μg mL^{-1} and *S. aureus*, MIC value: 50.99 μg mL^{-1}) and Gram-negative bacteria (*E. coli*, MIC value: 163.61 μg mL^{-1} and *S. typhimurium*, MIC value: 79.11 μg mL^{-1}) (Figure 19).[88] The anti-bacterial activity of the complex was suggested to arise from the unique hydroxo-bridged geometry of the complex along with its 2D hydrogen bonding molecular network.

Recently, Kargar and co-workers synthesized several new Cu^{II} complexes 45–48 from the corresponding bidentate Schiff-base ligands L27–L30 (Figure 20) and studied the effects of substituent groups on their anti-bacterial activities against *Staphylococcus aureus* (*S. aur*) and *Escherichia coli* (*E. coli*).[89] Compared to their parent ligands all of the metal complexes exhibited higher anti-bacterial activities against the bacterial species. The effect of substituent –OMe group was found to be very strong on antibacterial activities of both the ligands and the metal complexes. Whereas the respective MIC (μg mL^{-1}) values for the ligands L27–L30 against *E. coli* and *S. aur* were found to be 512 & 256, 256 & 128, 128 & 64 and 256 & 256, the values for the corresponding metal complexes 45–48 against the two bacterial species were observed as 128 & 32, 64 & 32, 64 & 32 and 64 & 64. Ligand L29 exhibited the highest antibacterial activities which were attributed to the position of the methoxy group (-OMe), which is a strong electron-donor substituent.

The methoxy group L29 is *para* to the hydroxyl group and is further away so it can more effectively form hydrogen bond(s) with the active centers of the cell constituents. On the other hand the strong internal hydrogen bond that can form between the closer position of the methoxy oxygen and the hydroxy group in L28 reduces the ligand's ability to form the effective hydrogen bonds with the active centers of the cell constituents. A similar trend of antibacterial activities was observed in the corresponding metal complexes 45–48, however, the higher activities of the metal complexes compared to those of the parent ligands were due to the reduction

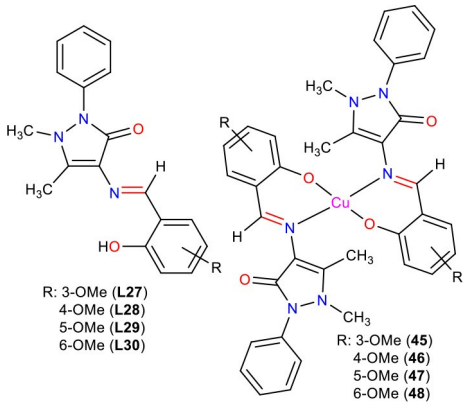

Figure 20. Structures of ligand L27–L30 and the corresponding Cu^{II} complex 45–48.[89]

of polarity of the central metal ions through the coordination with the Schiff base ligands thereby facilitating the interaction of the complexes with the cellular membranes.

Bhaskar group synthesized zinc-Schiff base complex 49 from the Schiff-base ligand L31 (Figure 21a–b).[90] Complex 49 showed good anti-bacterial activity against the clinical pathogen *Bacillus SP* (MIC value of 50 mg mL^{-1}). The anti-baceral activity of the complex 49 came from its ability to destroy the bacterial speicies or to prevent its growth through the generation of the reactive oxygen species (ROS), which caused oxidative stress and led to the damage of the cell membrane as well as DNA (Figure 21c).

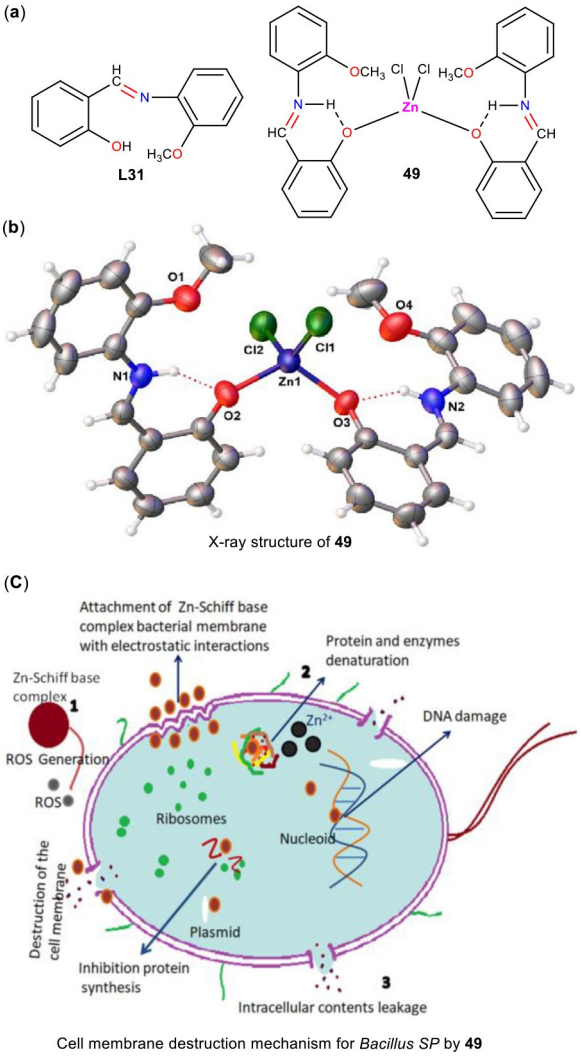

Figure 21. (a) Structures of ligand L31 and its Zn^{II} complex 49. (b) X-ray structure of complex 49 (Reproduced from Ref. [90]. Copyright (2021) Science direct. (c) Cell membrane destruction of *Bacillus SP* by 49 (Reproduced from Ref. [90]. Copyright (2021) Science direct).

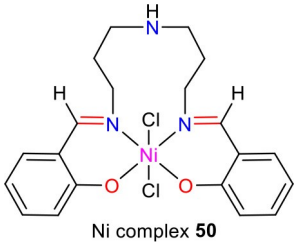

Figure 22. Strucutre of Schiff-base Ni complex 50.[91]

Teixeira and co-workers also performed anti-bacterial assay with Ni complex 50 (Figure 22) against *P. aeruginosa*, *S. aureus* and *E. coli*.[91] The complex didn't show any satisfactory activity against *S. aureus* and *E. coli* (MIC $\geq$ 1024 μg mL^{-1}) but exhibited activity against *P. aeruginosa* (MIC = 256 μg mL^{-1}).

2.2. Metal Complexes Exhibiting Anti-tumor and Anti-cancer Activities

Platinum-based cancer drugs (e,g. *cis*-platin) have long been used for the treatment of cancer patients.[92,93] However, due to their adverse side effects, the development of effective non-platinum drugs (based on metal ions such as Ru, Ir, Cu, Ni, Zn, Co, etc.) with much better anti-cancer properties than *cis*-platin has been carried out.[94–97]

Arunachalam and co-workers reported two cobalt(III) Schiff-base complexes, *trans*-[Co(salen)(DA)$_2$](ClO$_4$) **51** and *trans*-[Co-(salophen)(DA)$_2$](ClO$_4$) **52** (where salen: *N,N′*-bis(salicylidene)ethylenediamine **L32**, salopen: *N,N′*-bis(salicylidene)-1,2-phenylenediamine **L33**, DA: dodecylamine) (Figure 23).[61] The *in vitro* cytotoxicity of both complexes were tested against A549 (human small cell lung carcinoma). The respective IC$_{50}$ values of 80 μM and 65 μM of the complexes, **51** and **52** for A549 cell indicated that the *trans*-[Co-(salophen)(DA)$_2$](ClO$_4$) **52** complex was more effective than *trans*-[Co(salen)(DA)$_2$](ClO$_4$) **51**. Of the two complexes, the higher anti-cancer activity of **52** could be attributed to its higher DNA binding propensity (higher intrinsic binding constant, $K_b = 3.15 \times 10^4$ M^{-1}, and percentage of hypochromism, 36.81 %) than that of complex, **51** (intrinsic binding constant, $K_b = 1.31 \times 10^4$ M^{-1}, and percentage of hypochromism, 30.34 %).

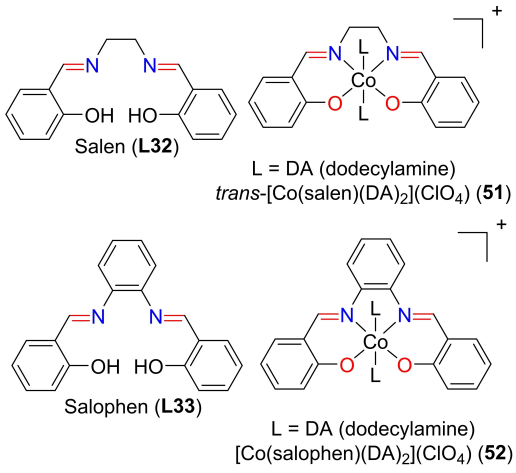

Figure 23. Structures of salen ligand **L32**, salophen ligand **L33** and their Co^{II} complexes **51**–**52**.[61]

This enhancement of stacking interactions between the salicylaldehyde aromatic moiety in *trans*-[Co(salophen)$(DA)_2$](ClO_4) **52** and DNA bases presumably arising from the presence of the additional aromatic phenyl ring in the Schiff-base ligand in the complex.

Wilson's group reported several bis(thiosemicarbazone) complexes of cobalt(III) with the general formula [Co(BTSC)$(L)_2$]NO_3 **53–55** (Figure 24) (where BTSC = diacetyl bis(thiosemicarbazone) (ATS) **L34**, pyruvaldehyde bis(thiosemicarbazone) (PTS) **L35**, or glyoxal bis(thiosemicarbazone) (GTS) **L36** where L = ammonia (NH_3) **53**, imidazole (Im) **54**, or benzylamine (BnA) **55**. Results proved that these complexes have the potential to become promising second generation anti-cancer pro-drugs.[98]

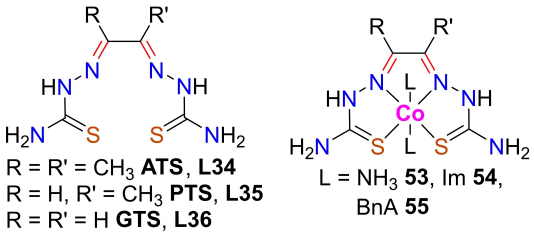

Figure 24. Structures of ligands, **L34–L36** and Co^{III} complexes **53–55**.[98]

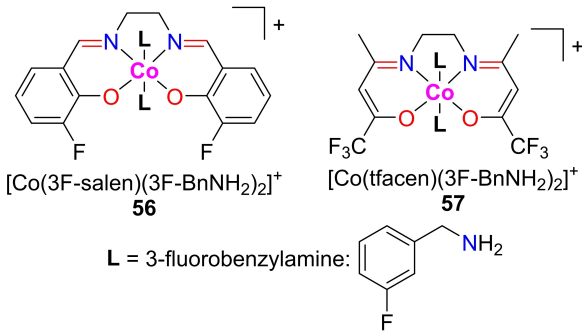

Figure 25. Structures of Co^{III} complexes **56–57**.[99]

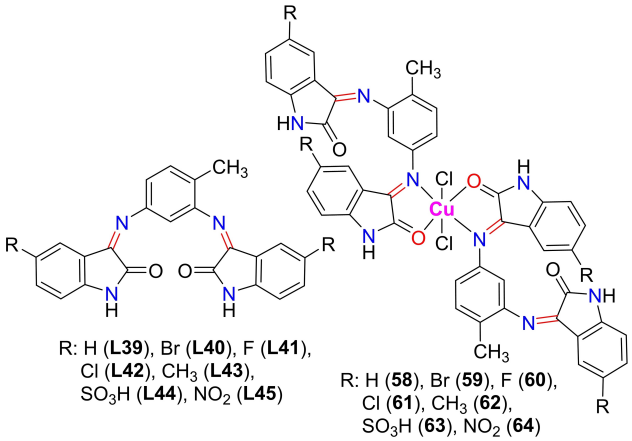

Figure 26. Structures of ligands, **L39–L45** and Cu^{II} complexes **58–64**.[100]

The Wilson group also synthesized Co^{III} Schiff-base complexes, [Co(3F-salen)$(3F\text{-}BnNH_2)_2]^+$ **56** and [Co(tfacen)$(3F\text{-}BnNH_2)_2]^+$ **57** bearing axial 3F-$BnNH_2$ ligands (where, 3F-salen: 3-fluorosalicylaldehyde ethylenediamine **L37**, tfacen: trifluoroacetylacetone ethylenediamine **L38** and 3F-$BnNH_2$: 3-fluorobenzylamine) (Figure 25).[99] The respective 50% growth inhibitory concentration (IC_{50}) values of 50 and 60 μM for the complexes against A549 lung cancer cells indicated that the complexes exhibited moderate anti-cancer activity. This activity might involve a ligand exchange mechanism in which the axial ligands played an important role.

Pervez, Iqbal and co-workers studied the anti-cancer activities against lung carcinoma (H157) cells in the presence of some novel isatin-derived bis-Schiff-bases, **L39–L45** and the derived Cu^{II} complexes **58–64** (Figure 26).[100] Among the Schiff-bases, halo-substituted compounds **L35–L37** (containing electron-withdrawing halogen functional groups at position-5 of the isatin moiety) exhibited higher inhibitions of H157 cells (IC_{50} values ranging from 2.32 ± 0.11 to 2.99 ± 0.15 μM) than those of the other Schiff-bases.

Bromo-substituted compound **L40** exhibited the highest anti-cancer activity (IC_{50} value of 2.32 ± 0.11 μM) among a number of isatin-derived imines most probably due to its higher degree of lipophilicity which enabled it to bind with the receptor sites by crossing the lipid membrane. Enhancement of activity was observed for Cu^{II} complexes, **58–64** synthesized from the Schiff-bases **L39–L45** (Table 3). The highest inhibition against H157 was observed for complex **61** (IC_{50} value of 1.29 ± 0.06 μM) containing electron-withdrawing chloro group at position-5 of the isatin scaffold, whereas complex **59** having higher lipophilicity than **61** exhibited less inhibition (IC_{50} value of 1.54 ± 0.04 μM).

Cu^{II} complexes synthesized from 6-methyl-2-oxo-1,2-dihydroquinoline-3-carboxaldehyde-4(*N*)-substituted Schiff-bases also showed significant activity against human skin cancer cell line (A431).[101] Rigamonti and co-workers studied anti-cancer activities of the Schiff-base Cu^{II} complexes [Cu(^{OMe}L)(Cl)] **65**, [Cu(^{H}L)(Cl)] **66** and [Cu(^{NO2}L)(Cl)] **67** (where, ^{OMe}L, ^{H}L and ^{NO2}L are Schiff-base ligands) against three difficultly diagnosed and poorly curable cancer cells.[102] The inhibitory activities (IC_{50}) of the complexes (Figure 27), **65–67** were evaluated against human triple-negative breast cancer cells (MDA-MB-231), human glioblastoma cells (U-87) and human androgen independent prostate carcinoma cells (PC-3). The time-dependent IC_{50} values (μM) of the complexes against the three cancer cells

Table 3. Cytotoxicity of complexes **58–64** against lung carcinoma (H157) cell. (data taken from Ref. [100]).

Compounds	R	H157 IC_{50} (μM)
58	H	1.93 ± 0.07
59	Br	1.54 ± 0.04
60	F	1.47 ± 0.03
61	Cl	1.29 ± 0.06
62	CH_3	2.87 ± 0.18
63	SO_3H	2.32 ± 0.05
64	NO_2	2.67 ± 0.23
Vincristine		1.03 ± 0.23

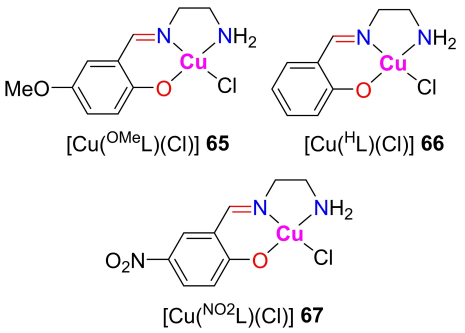

Figure 27. Structures of Cu^{II} complexes, **65–67**.[102]

were compared with those of healthy human endothelial cells (HUVEC) (Table 4). Among the complexes, [Cu(^{NO2}L)(Cl)] **67** exhibited the highest activities against all three cancer cell lines. The two- to-four-fold cytotoxicity enhancement of complex [Cu(^{NO2}L)(Cl)] **67** against the cancer cells compared to the other two complexes, could be attributed to the presence of the nitro (NO_2) group.

All three complexes exhibited high inhibitory activities against the MDA-MB-231 cells as follows: ([Cu(^{NO2}L)(Cl)] **67** > [Cu(^{OMe}L)(Cl)] **65** > [Cu(^{H}L)(Cl)] **66**) (Table 4). The higher capabilities of the complexes to generate selective intracellular reactive oxygen species (ROS) and the larger DNA fragmentation abilities in contact with MDA-MB-231 cells enabled the complexes to manifest higher activities against the breast cancer cells compared to others. Complex, [Cu(^{NO2}L)(Cl)] **67** showed the highest cytotoxicity against the target cells due to the presence of nitro (NO_2) group as it was suspected to facilitate the DNA interaction with nuclease activity when in contact with the cells. Compared to the healthy endothelial HUVEC cells, a substantial selectivity index (3.6) was observed in the case of [Cu(^{NO2}L)(Cl)] **67** which is quite promising as a potential anti-cancer agent especially against the MDA-MB-231 cells.

Cu^{II} complex, $[Cu_2(LH)_2](ClO_4)_2$ **68** was synthesized from the Schiff-base ligand, HL (**L46)** (Figure 28a) and showed strong binding affinity with DNA (intrinsic binding constant $K_b = 6.16 \times 10^7\ M^{-1}$).[103] The complex showed significant cytotoxicity against human colon cancer cell line (HCT 116), human liver cancer cell line (HepG2), murine melanoma cell (tumor cell) line (B16F10) and normal kidney epithelial cells (HEK 293), whereas

Table 4. Time-dependent IC_{50} values (μM) of **65** and **67** against MDA-MB-231, U-87 and PC-3 malignant human cell lines together with healthy HUVEC cell. (data taken from Ref. [102]).

		MDA-MB-231	U-87	PC-3	HUVEC
$t = 24$ h	65	31.0	64.8	61.8	97.1
	67	17.9	60.5	131.7	50.8
$t = 48$ h	65	20.1	38.6	45.2	45.2
	67	10.1	22.2	18.8	46.0
$t = 72$ h	65	17.3	40.5	42.2	52.7
	67	8.1	20.7	10.7	28.6

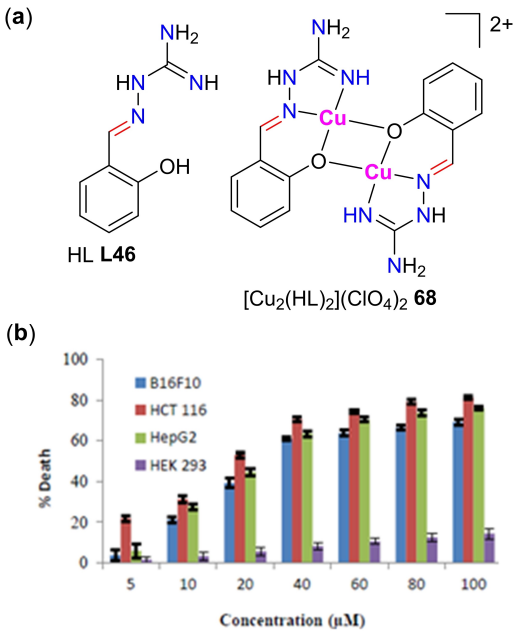

Figure 28. (a) Structures of ligand HL (**L46**) and its Cu^{II} complex **68**. (b) Activity of complex **68** (MTT assay, concentrations (5-100 μM)) against different type of cells (1 x 10^6 cells/mL) (Reproduced from Ref. [103]. Copyright (2020) RSC).

the highest activity was observed against the colon cancer cell line HCT116 (Figure 28b).

Interestingly, $[Cu_2(LH)_2](ClO_4)_2$ **68** exhibited the lowest toxic effect against the HEK 293. Khan's group studied the cytotoxicity of Cu^{II} complexes, **69–71** (Figure 29) which exhibited concentration-dependent cytotoxic profiles against the cultured human breast cancer MCF-7 cell lines.[63] The anti-cancer activity of the complexes were higher than that of the Schiff-base ligand, which confirmed the important role of the Cu^{II} ion in the potency of the complexes. The highest anti-cancer activity of complex **71** was attributed to the strong interaction of its planar "phen" co-ligand with DNA base pairs resulting in cell death. The Cu(II) complexes, **69–71** were observed to exert low cytotoxicity against HEK293. Chiral Cu^{II} complexes were also reported to demonstrate toxic effect on epidermoid human cancer cell line (A431).[80]

Neelakantan's group synthesized several mononuclear complexes $Cu(L^1)$ **72**, $Cu(L^2)$ **73**, $Ni(L^1)$ **74** and $Ni(L^2)$ **75** containing Schiff-base ligands H_2L^1 (**L48**) and H_2L^2 (**L49**) (Figure 30).[104] Complexes **72–75** were found to have higher binding affinities with the respective cell DNA binding constants ($K_b = 4.88 \times 10^4\ M^{-1}$; 5.98×10^4; 4.26×10^4 and 5.38×10^4), than those observed for the ligands ($K_b = 1.80 \times 10^4\ M^{-1}$ for **L48** and 1.91×10^4 for **L49**). Furthermore, these complexes acted as efficient DNA nucleases which resulted in their abilities to exert cytotoxicity [IC_{50} (μM) values: 22.52 ± 0.49 for **L48**; 19.86 ± 0.62 for **L49**; 12.15 ± 0.04 for (**72**); 11.02 ± 0.16 for **73**; 15.11 ± 0.13 for **74** and 13.63 ± 0.09 for **75**] against human cervical carcinoma cell line (HeLa). Although the anti-cancer activity of the complexes against HeLa was found to be lower than that

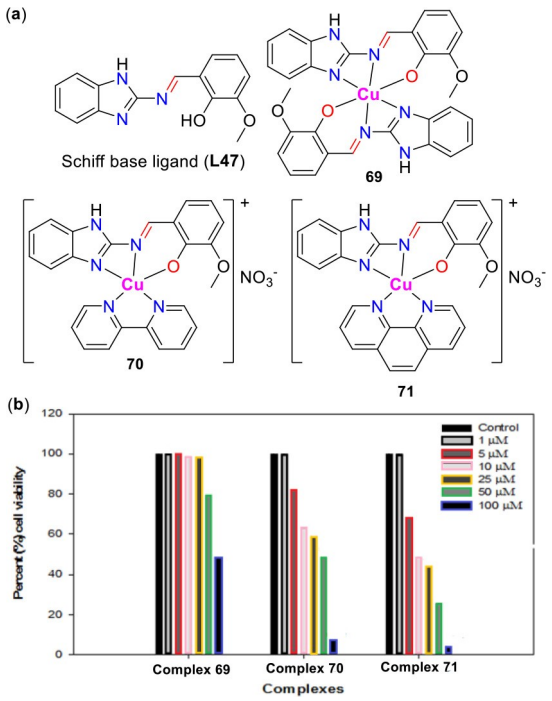

Figure 29. (a) Structures of Schiff-base ligand **L47** and its Cu^{II} complexes, **69–71**.[63] (b) Concentration-dependent cytotoxicity of the complexes **69–71** against human breast cancer MCF-7 cell lines (Reproduced from Ref. [63]. Copyright (2019) Nature Publication).

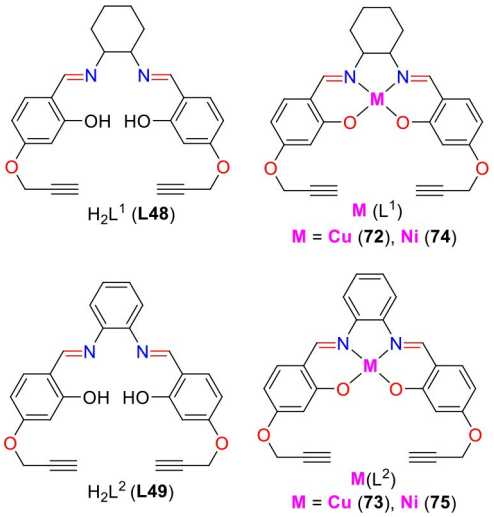

Figure 30. Structures of Schiff-base ligands **L48–L49** and their Cu^{II} and Ni^{II} complexes, **72–75**.[104]

observed for the well-known drug *cis*-platin ($IC_{50} = 8.67 \pm 0.04$ μM), the complexes could be used as potential anti-tumor agents due to their lower side effects compared to cisplatin.

The Zn^{II} complex, $[Zn^{II}L(H_2O)Cl]_x5H_2O$ **76** was synthesized from the Schiff-base ligand, HL (**L50**)) (Figure 31) and was tested for anti-tumor activity against colon carcinoma HCT-116 cells as well with the mouse myelogenous leukemia carcinoma (M-NFS-60) cell line.[73] Alaghaz and co-workers obtained very

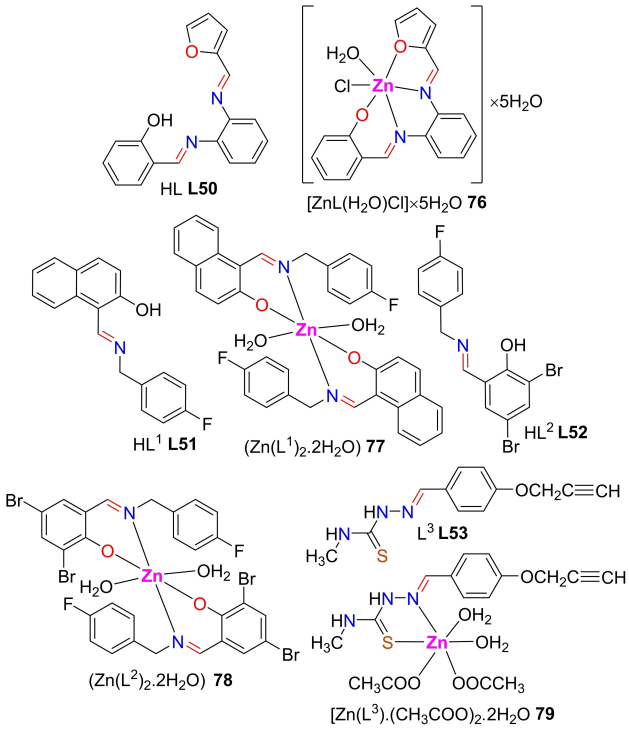

Figure 31. Structures of Schiff-base ligands, **L50–L53** and its Zn^{II} complexes, **76–79**.[73,76,85]

high cytotoxicity levels for the complex **76**, against the HCT-116 and M-NFS-60 cell lines (IC_{50} = 17.61 and 17.53 μg mL^{-1}, respectively). Devi *et al.* studied the *in vitro* anti-cancer activities of the Zn^{II} complexes, $Zn(L^1)_2{\cdot}2H_2O$ **77** and $Zn(L^2)_2{\cdot}2H_2O$ **78** (Figure 31) against the following malignant tumour cell lines: Human lung carcinoma cell line A549, Human breast carcinoma cell line MCF7 and Human prostate carcinoma cell line DU145.[76]

Complex, **78** which incorporated the Schiff-base ligand, HL^2 (**L52**), displayed higher activities against A549, MCF7 and DU145 cancer cell lines (with corresponding IC_{50} values of 6.6, 4.3 and 5.8 μM, respectively) than those of complex **77** which incorporated Schiff-base ligand, HL^1 **L51**, (with corresponding IC_{50} values of 8.6, 6.7 and 10.7 μM, respectively), against the three cancer cells. The authors also reported significant anti-cancer activities against the aforementioned three cancer cells for another Zn^{II} complex, $Zn(L^3){\cdot}(CH_3COO)_2{\cdot}2H_2O$ (**79**) which was synthesized from ligand, L^3 **L53** (Figure 31) with respective IC_{50} values of 10.6, 13.4 and 12.9 μM.[85] The cytotoxic selectivity of the Zn^{II} complexes **77–79**, was quite high since all showed very low cytotoxicity against the normal human lung cell line (MRC5).

Coordination of Schiff-base ligands with metal ions can increase the anti-cancer activity of the metal complexes. Prabhakaran *et al.* witnessed up to six times higher anti-cancer activities of Ru^{II} complexes, **80–83** compared to their parent coumarin-appended thiosemicarbazone ligands, H_2L^{1-4} (**L54–L57**) (Figure 32) against the MCF-7 and A549 cell lines.[75] The anti-cancer activity of the complexes increased up to eight

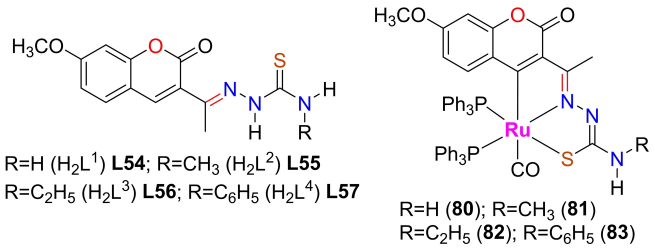

Figure 32. Structures of ligand H_2L^{1-4} (**L54–L57**) and their Ru^{II} complexes, **80–83**.[75]

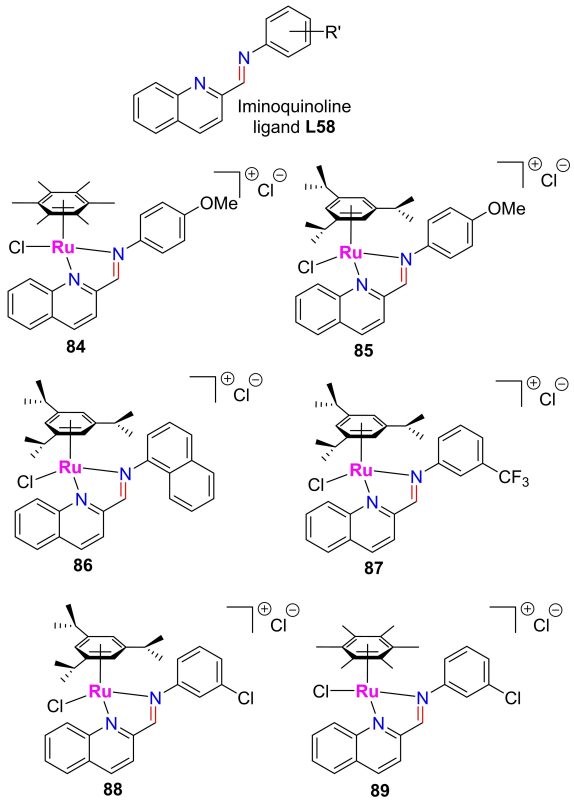

Figure 33. Structures of iminoquinoline ligand **L58** and its Ru^{II} complexes **84–89**.[106]

times higher than *cis*-platin. The ability of the complexes to intercalate the DNA base pairs and/or their free radical-scavenging activity, might be the key point to exhibit their anti-cancer activities. The order of activity of the compounds was observed to be varied depending on the substituent at the *N*-terminal nitrogen. The anti-proliferative activity of the compounds against both MCF-7 and A549 cell lines was as follows: **82** > **81** > **80** > **83** > H_2L^3 (**56**) > H_2L^2 (**55**) > H_2L^1 (**54**) > H_2L^4 (**57**). Due to the presence of more electron donating ethyl group at *N*-terminal nitrogen, Ru^{II} complex **82** exhibited the highest anti-cancer activity. The IC_{50} values for Ru^{II} complexes, **80–83** against MCF-7 cell line were obtained as 2.86 ± 0.17, 2.62 ± 0.07, 2.53 ± 0.10 and 3.02 ± 0.05 μM, respectively. The corresponding values against A549 are 2.96 ± 0.07, 2.93 ± 0.07, 2.37 ± 0.04 and 3.05 ± 0.12 μM, respectively. The cytotoxicity of *cis*-platin against MCF-7 and A549 was lower than that of the compounds (ligands and their complexes) with respective IC_{50} values of 16.79 ± 0.08 and 15.10 ± 0.05 μM, respective;y. The compounds were very selective as anti-cancer agents, and showed no significant toxicity on the human normal keratinocyte cells (HaCaT).

Several other Ru complexes exhibiting potential anti-tumor activities were also reported. Aziz group obtained weak to moderate anti-tumor activities against liver carcinoma (HepG2), breast carcinoma (MCF7) and colon carcinoma (HCT-116) cell lines.[105] Gaiddon, Ang and co-workers synthesized several anti-cancer ruthenium-arene Schiff-base complexes, **84–89** (Figure 33) and demonstrated their p53-independent cytotoxicity.[106] They discussed the structural features of the complexes which were essential for following the p53-independent mode-of-action. p53 is a key tumor suppressor gene in key cellular processes and in cancer therapy. Gaiddon's group showed that the structural arrangement involved in iminoquinoline ligand (**L58**) from which all the Ru-complexes, **84–89** were prepared, was the key point so that these complexes exhibited anti-cancer activities against human colorectal carcinoma cells (HCT116), human colorectal adenocarcinoma cells (SW480), human gastric adenocarcinoma cells (AGS) and human gastric carcinoma cells (KATOIII) through the p53-independent mechanism. Increased activity of the complexes was observed with increasing hydrophobicity. Complexes **84–89** exhibited remarkable anti-cancer activities against HCT116, SW480, AGS and KATOIII (Table 5) and were found to remain unchanged in the presence of p53-inhibitors.

Liu *et al.* pointed out an energy-dependent cellular uptake mechanism for the Ru complexes.[107] Complexes, **90–93** synthesized from Schiff-base ligands, **L59–L62** (Figure 34)

Table 5. IC_{50} values of Ru^{II} complexes, **84–89** against HCT116, SW480, AGS and KATOIII cells. (data taken from Ref. [106]).

Compounds	IC_{50} (μM)[a] HCT116	SW480	AGS	KATOIII
84	5.76 ± 1.22	34.7 ± 19.3	3.04 ± 0.91	13.7 ± 5.0
85	1.19 ± 0.12	4.07 ± 1.35	1.01 ± 0.07	1.22 ± 0.24
86	3.48 ± 0.36	5.32 ± 2.09	1.16 ± 0.28	1.86 ± 0.24
87	6.87 ± 1.11	13.9 ± 5.5	3.07 ± 0.72	3.89 ± 0.15
88	5.76 ± 013	11.0 ± 4.7	2.76 ± 0.82	3.28 ± 1.12
89	3.05 ± 026	16.0 ± 6.1	1.95 ± 0.40	2.22 ± 0.35

[a] IC_{50} values: Concentration of Ru^{II} complexes, **84–89** required to inhibit 50% of cell growth, measured by MTT assay after 48 h of incubation.

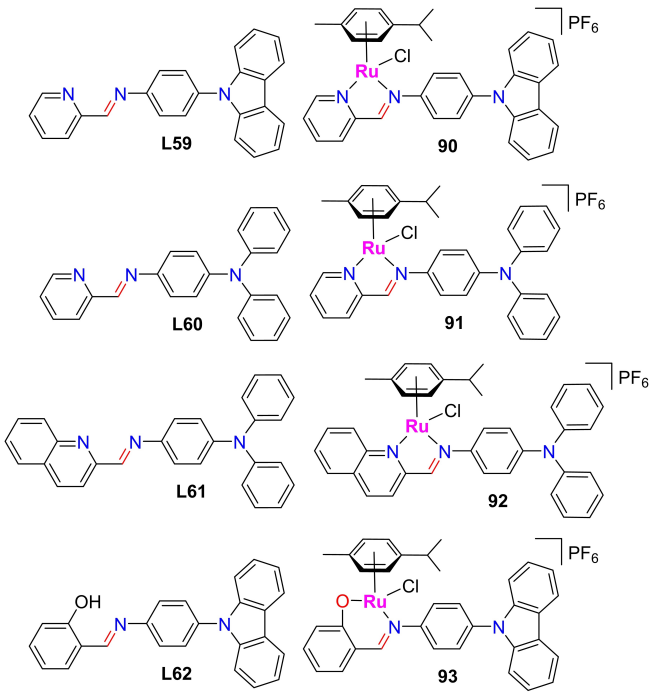

Figure 34. Structures of Schiff-base ligands, **L59**–**L62** and their Ru complexes, **90**–**93**.[107]

promoted apoptosis in tumor cells through lysosomal damage. They also had potential to inhibit metastasis. The highest antitumor activity of the complexes was observed against A549 and it was even higher than the widely used clinical antitumor drug, *cis*-platin. The enhanced activity of the complexes against A549 was due to the coordination of the Schiff-base chelating ligands, **L59**–**L62** with Ru metal ions. The compounds followed an antitumor mechanism of oxidation involving an increase of intracellular reactive oxygen species (ROS) levels, a decrease of mitochondrial membrane potential (MMP), and the catalytic oxidation of the coenzyme nicotinamide-adenine dinucleotide (NADH).

The better electron donor capacity of **L61** due to the introduction of more phenyl groups in **L61**, was responsible for the highest activity of complex **92** (IC_{50} value of 2.8 ± 1.0 μM) which was also confirmed through the natural population analysis (NPA). This antitumor activity was actually 8 times higher than *cis*-platin. The activity of the N N ligand-based compounds (**90**, **91**, and **92** with respective IC_{50} values: 8.0 ± 0.07, 8.2 ± 2.5, and 2.8 ± 1.0 μM, respectively) was higher than the O N based one (**93**, IC_{50} value: 17.8 ± 3.1 μM). Moreover, the anti-tumor activity of the complexes was found to increase with the lipid solubility since the log $P_{O/W}$ (partition coefficient in oil/water) value of each complex **90**–**93** was 0.42, 0.41, 0.75, and 0.35, respectively.

Schiff-base Pd^{II} complexes were also found to have potential to exhibit significant anti-cancer activities against different cancer cells. Petrović and co-workers reported Pd^{II} complexes, **94**–**95** synthesized from Schiff-base ligands **L63** and **L64** (Figure 35) showing significant cytotoxic effect on

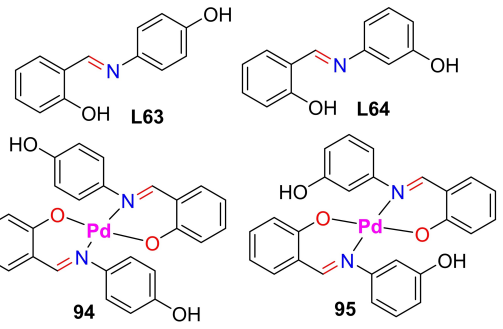

Figure 35. Structures of Schiff-base ligands, **L63**–**L64** and their Pd^{II} complexes **94**–**95**.[108]

MDA-MB-231 and HCT-116 cells with respective IC_{50} values in the range of 7.2 to 55.6 μM and 0.6 to 17.1 μM whereas their ligands **L63** and **L64** did not exert such significant cytotoxic effects.[108]

Pd^{II} complex **96** synthesized by the Prabhakaran group from 3-acetyl-8-methoxycoumarin Schiff-base ligand **L65** (Figure 36) provided high anti-cancer activity against MCF-7 and A549 cancer cell lines with IC_{50} values of 5.20 ± 0.15 μM and 5.09 ± 0.13 μM respectively, which were higher than *cis*-platin (corresponding IC_{50} values of 16.79 ± 0.08 μM and 15.10 ± 0.05 μM).[109]

The cytotoxicity of Pd complex **97** and Pt complex **98** (Figure 37) were studied by Onani's group against the human cell lines Caco-2 (colon), HeLa (Cervical), Hep-G2 (Hepatocellular Carcinoma/liver cancer), MCF-7 (breast cancer), PC-3 (prostate), and MCF-12 A (non-cancer breast).[110] The complexes were highly toxic to the cancer cells. A greater than 80% reduction of cell viability was recorded by the most cytotoxic complex **97**, in the six cell lines, whereas selective toxicity was obtained with the complex **98** against all of the cancer cell lines with reduction of cell viability by 60% or more, but the viability of the noncancerous MCF-12 A cells was not found to be affected. Moreover, complex **98** demonstrated strong DNA intercalation activity with a binding constant of $8.049 \times 10^4\ M^{-1}$ which

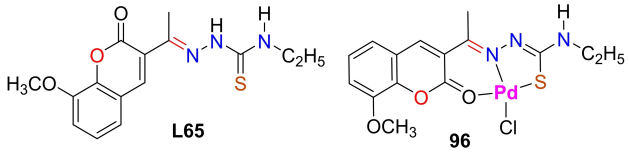

Figure 36. Structures of Schiff-base ligand **L65** and its Pd^{II} complex **96**.[109]

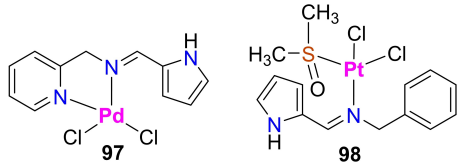

Figure 37. Structures of Pd^{II} complex **97** and Pt^{II} complex **98**.[110]

suggested that complex **98** can be a potential candidate for cancer treatment.

Abdulla and co-workers studied the cytotoxicity and apoptotic activity of $CdCl_2(C_{14}H_{21}N_3O_2)$ complex **99** (Figure 38a) on colon cancer HT-29 cells.[111] They obtained anti-cancer activity of complex **99** against the colon cancer HT-29 cell lines with an IC_{50} value of $2.57 \pm 0.39\ \mu g\ mL^{-1}$ after 72 h of treatment, through the activation of the mitochondrial pathway (both intrinsically confirmed through the subsidence of the mitochondrial membrane potential (MMP) and the elevated release of cytochrome c from the mitochondria to the cytosol) and extrinsically (confirmed through the activation of caspase-9 and −8 after suppression of the NF-κB translocation signaling pathway to the nucleus) in the cancer cells whereas no cytotoxic effect of the complex was observed against normal colon cell line (CCD 841).

Taha *et al.* recorded the anti-cancer activity of a bibasic tetradentate Schiff-base ligand H_2L^1 **L66** and a La^{III} complex **100** in the nanoscale (Figure 38b) against human epithelial colorectal adenocarcinoma cells (Caco-2).[112] Against the Caco-2 cells line, the inhibition percentage of 63.42 and the IC_{50} value of $0.4571\ \mu g\ mL^{-1}$ for **L66** was observed. A dramatic increase in the anticancer activity of **L66** to the level of 72.13% and IC_{50} $0.3772\ \mu g\ mL^{-1}$ was observed for the nano La^{III} complex **100**.[112] The enhancement of the anti-cancer activity of the complex might be related to the presence of elemental La synthesized in the nanoscale.

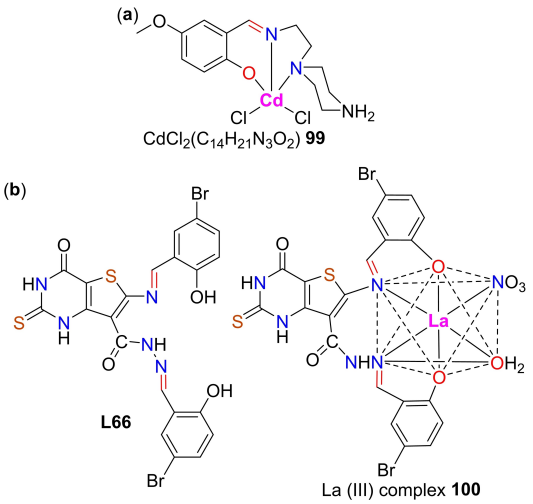

Figure 38. Structures of (a) Cd^{II} complex **99**[111] and (b) Schiff-base ligand **L66** and the La^{III} complex **100**.[112]

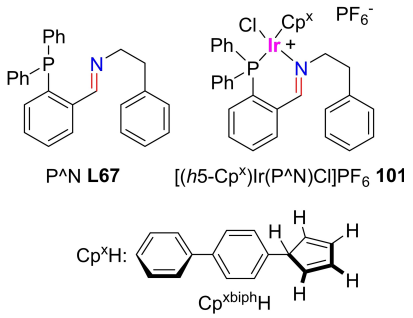

Figure 39. Structures of Schiff-base ligand **L67** and its Ir^{III} complex **101**.[115]

The ability of the Schiff-bases and their metallic complexes in inducing apoptosis pathways is thought to be responsible for their anti-cancer potential.[113–114] Metallic complexes of Schiff-bases are greater apoptosis inducers than the Schiff-bases themselves. Guo, Liu and co-workers studied the anti-cancer activity of the half-sandwich iridium(III) complex **101** (synthesized from phosphine-imine ligand **L67**) (Figure 39) against A549 cancer cells.[115] The anti-cancer activity of complex **101** ($IC_{50} = 4.7\ \mu M$) was approximately 4.5-fold higher than that of *cis*-platin ($IC_{50} = 21.30\ \mu M$). This enhanced activity was attributed to the coordination between iridium(III) and the coordinating atoms in complex **101**. The complex was suggested to cause the disruption of lysosomes in A549 cancer cells which caused the cell death. The mechanism involved the disruption of MMP, generation of ROS, cell apoptosis and necrosis.

2.3. Metal Complexes Exhibiting Antioxidant Activities

Antioxidants at low concentrations inhibit or delay the oxidation of oxidizable substrates/molecules. In cellular process, where the destruction of cells occurs through the chain reactions of free radicals (produced through the oxidation reaction), the antioxidants interrupt the oxidative chain reactions by preventing the initiation or propagation steps. Antioxidants also prevent the risk of several chronic diseases (e.g. cancer and heart disease) when they are present in food. Schiff-bases and their metal complexes are excellent antioxidants. Several compounds exhibiting significant antioxidant properties have been reported. The stable free-radical DPPH• (2,2-diphenyl-1-picrylhydrazyl) radical is commonly employed for the assay of antioxidant activities of selected compounds across a short time scale.

Pramanik, Chakrabarti and co-workers studied the half maximal effective concentration (EC_{50}) values of DPPH• scavenging activities of Schiff-base ligand **L7** and its mononuclear dioxomolybdenum(VI) complexes **9** and **102** which were then compared with the activity of ascorbic acid. Ligand **L7** showed remarkable antioxidant activity compared to that of ascorbic acid which was even higher than the activity of complexes **9** and **102** (Figure 40).[68] Prabhakaran's group also studied the antioxidant activities of coumarin-appended thiosemicarbazone ligands, **L54**–**L57** and their corresponding complexes, **80**–**83** (Figure 32) based on the DPPH free radical scavenging activities of the compounds, as well as using the phosphomolybdate method.[75] The total antioxidant activities of the compounds expressed as the number of equivalents of ascorbic acid followed the order: **82** > **81** > **80** > **83** > **L56** > **L55** > **L54** > **L57** > ascorbic acid. The IC_{50} values (μM) of the tested compounds on DPPH• radical were found to be as follows: 83.17 ± 1.50 (**L54**), 80.75 ± 1.34 (**L55**), 67.28 ± 1.44 (**L56**), 91.21 ± 1.54 (**L57**), 7.13 ± 0.23 (**80**), 6.75 ± 0.18 (**81**), 5.28 ± 0.24 (**82**), 7.39 ± 0.14 (**83**) and 98.72 ± 1.50 (ascorbic acid).

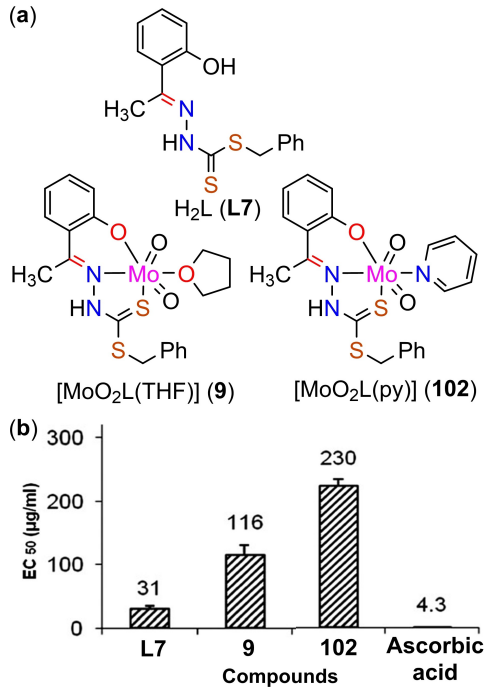

Figure 40. (a) Structures of dioxomolybdenum (VI) complex **102** and (b) Plot showing EC_{50} values (μg mL^{-1}) of ligand **L7** and complexes **9** and **102** (Reproduced from Ref. [68]. Copyright (2015) RSC).[68]

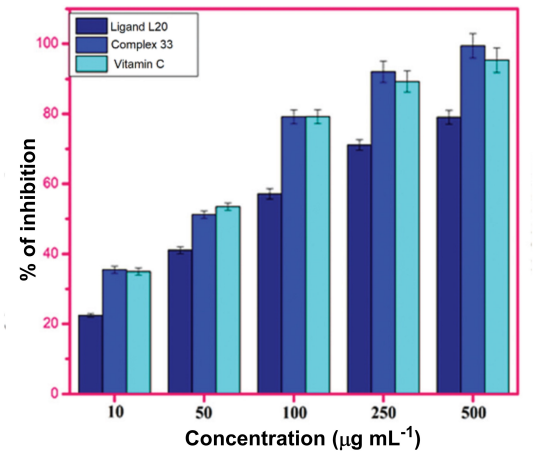

Figure 41. Total antioxidant potential of the chitosan Schiff-base ligand **L20** and its Zn^{II} complex **33** (Reproduced from Ref. [82]. Copyright (2019) RSC).

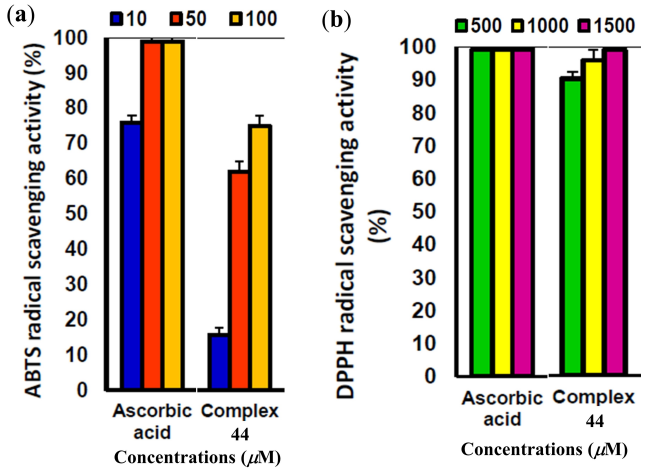

Figure 42. (a) ABTS radical scavenging activity of complex **44** taking ascorbic acid as standard and (b) DPPH scavenging activity of complex **44** taking ascorbic acid as standard (Reproduced from Ref. [88]. Copyright (2020) ACS).

Using the DPPH• scavenging method, Pawar and co-workers also studied the antioxidant activity of Schiff-base ligands **L17** and **L18** (Figure 12). The obtained free radical scavenging activity (IC_{50} value of 92.20 μM mL^{-1} for **L17** and that of 130.73 μM mL^{-1} for **L18**) was comparable to that of the standard antioxidant ascorbic acid (IC_{50} value of 74.06 μM mL^{-1}).[77] Sithique and co-workers studied the total antioxidant activities of chitosan Schiff-base ligands **L20**–**L21** and their Zn^{II} complexes **33**–**34**.[82] Among the compounds, chitosan Schiff-base ligand **L20** and its Zn^{II} complex **33** exhibited the highest percentage of inhibition at 79.06 ± 2.0% and 99.43 ± 3.2%, respectively, when compared to ascorbic acid (Figure 41). Zn^{II} complex **33** showed higher scavenging activity than its parent ligand **L20**.

Generally, the species capable of donating a hydrogen atom are effective in radical scavenging and showed efficient antioxidant ability.[116] The dinuclear Zn^{II} complex, $[Zn_2(HL^1H)_2(OH)I_2]I$ **44** synthesized by Das and co-workers from the Schiff-base ligand H_2L^1 (**L26**) (Figure 19) showed high antioxidant activity which was confirmed through its high scavenging effect on DPPH• and ABTS• (2,2′-azino-bis(3-ethylbenzothiazoline-6-sulfonic acid)) radicals (Figure 42).[88] The dimeric structure of complex **44** containing two protonated amino groups was responsible for its ability to liberate protons in close proximity to DPPH• radical leading to high radical scavenging activity. The ample positive charge density due to the presence of two Zn^{II} ions, was responsible to attract ABTS• radical.

Buldurun and co-workers also utilized DPPH• and ABTS• radicals scavenging methods to study the antioxidant activities of Schiff-base ligand **L68** along with its Ru^{II} and Ni^{II} complexes **103**–**104** (Figure 43a).[117] All of the compounds demonstrated effective antioxidant activities. DPPH• radical scavenging percentages of ligand **L68** and its metal complexes **103** and **104** at the same concentration (30 μg mL^{-1}) were observed as 0.8 ± 0.1, 69.2 ± 17.4 and 16.2 ± 4.2, respectively, whereas the percentage for ascorbic acid was 63.6 ± 18.9. On the other hand, ABTS• radical scavenging percentages for the compounds at the same concentration (30 μg mL^{-1}) followed the order 93.5 ± 2.9 (ascorbic acid), 82.6 ± 14.3 (**103**), 77.9 ± 15.6 (**L68**), and 75.7 ± 16.1 (**104**), respectively.

Abdel-Satar's group obtained higher antioxidant activity for the Schiff-base ligand **L69** (73.36% of inhibition at concentration of 0.009 mg mL^{-1}) compared to its Cu^{II} complex, **105** (65.95% of inhibition at concentration of 0.009 mg mL^{-1}) (Figure 43b).[118] Zoubi, Ko and co-workers showed that the presence of electron donor groups such as hydroxyl moiety in Schiff-base might affect the DPPH radical-scavenging activity of the Schiff-base and its metal complexes.[119]

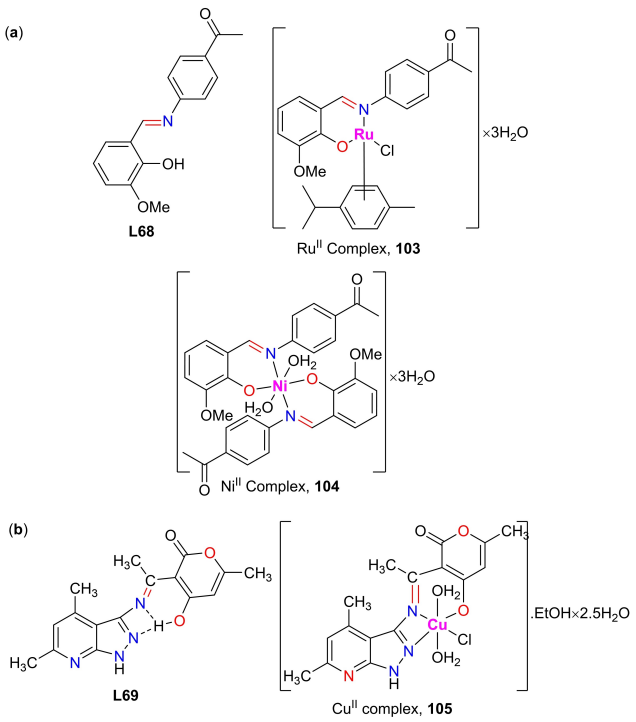

Figure 43. Structures of (a) Schiff-base ligand **L68** and its Ru^{II} and Ni^{II} complexes **103–104**[117] and (b) Schiff-base ligand **L69** and its Cu^{II} complex **105**.[118]

2.4. Metal Complexes Exhibiting Anti-inflammatory Activities

The symptoms of inflammatory process such as pain, edema, tenderness and redness result from the production of several chemical mediators like leukotrienes (LTs), histamine, HETEs, and prostaglandins. Prostaglandins, the major mediators of pain sensitization, and hyperpyrexia,[120] are generated from the arachidonic acid (being hydrolyzed by the action of cyclooxygenases enzymes) which is liberated from cell membrane phospholipids by the hydrolytic effect of the enzyme phospholipase, A2. On the other hand, leukotrienes (LTs) which are the primary mediators of inflammation development (through capillary permeability, chemotaxis of inflammatory mediators and extravasation of white blood cells)[120,121] are also produced from the arachidonic acid (being hydrolyzed by the action of lipoxygenases enzymes).[122] Substances through the inhibition of phospholipase A2 or cyclooxygenases may relieve pain and/or decreases body temperature whereas by inhibiting lipoxygenases, substances may inhibit inflammation alone. On the other hand, by inhibiting phospholipase A2 alone or with lipoxygenases and cyclooxygenases enzymes, substances may inhibit inflammation, pain and decrease body temperature.[123]

Complexes **69** and **71** (Figure 29a) synthesized by Khan's group exhibited significant anti-inflammatory effects which were dose-dependent and lasted up to 4 h after carrageenan injection.[63] They showed the anti-inflammatory effect at 100 mg/kg which might be accomplished by inhibiting both LTs and prostaglandins originated from the inhibition of either both cyclooxygenase and lipoxygenases enzyme families or phospholipase A2. On the other hand, through the probable inhibition of only cyclooxygenases enzymes, complex **70** produced only short significant anti-inflammatory effect at 100 mg/kg. Starting from 60 min, complexes **69** and **71** relieved pain till 120 min but complex **70** didn't show any significant inhibition at 120 min. Interestingly, complex **70** (at a dose of 50 mg/kg) was more effective than complexes **69** and **71** (at a dose of 100 mg/kg) in decreasing body temperature.

Sithique and co-workers showed that the incorporation of metal into hydrazone derivatives could give rise to potential anti-inflammation drug exhibiting better inhibition than the standard drug diclofenac sodium (Figure 44).[82] The research group utilized the bovine serum albumin (BSA) denaturation technique[124] to study the anti-inflammatory behavior of the hydrazone incorporating *O*-carboxymethyl chitosan Schiff-bases, **L20–L21** and their Zn^{II} complexes, **33–34** (Figure 14). The respective percentage of inhibition for **L20–L21** and their Zn^{II} complexes, **33–34** at the maximum concentration of 500 mg mL^{-1} were found as 78.16 ± 2.0%, 73.45 ± 1.9%, 95.31 ± 3.1% and 82.48 ± 2.1%.

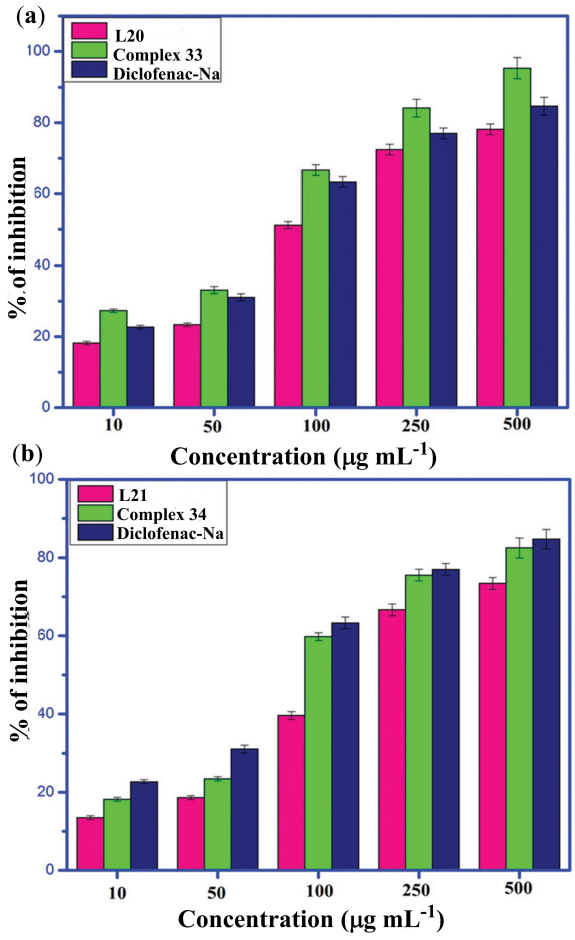

Figure 44. Anti-inflammatory studies of the (a) chitosan Schiff-base ligand **L20** and its Zn^{II} complex **33**, and (b) chitosan Schiff-base ligand **L21** and its Zn^{II} metal complex **34** (Reproduced from Ref. [82]. Copyright (2019) RSC).

2.5. Metal Complexes Exhibiting Other Therapeutic, Medicinal and Biological Activities

Schiff-base metal complexes can also find various other therapeutic, medicinal and biological applications. Co^{III} Schiff-base complexes 51 and 52 synthesized from Schiff-base ligands L32 and L33 (Figure 23) by Arunachalam and co-workers, showed remarkable anti-angiogenic potential in chicken chorioallantoic membrane (CAM) assay.[61] Pearce, Peterson and co-workers synthesized the Co^{II} complex, $Co^{II}N_4$[11.3.1] 106 (Figure 45) which was found to have potential to protect against azide intoxication.[125] Jurisson's group studied Schiff-base metal complexes as potential candidates for therapeutic nuclear medicine.[126] Khan's group reported that Cu complexes 69–71 (Figure 29a) showed significant binding affinities with human serum albumin (HSA).[63] Arjmand's group obtained promising *t*RNA binding interactions with enantiomeric amino acid Schiff-base Cu^{II} complexes, 107–110 (Figure 45).[127] Complex 68 synthesized by Corbella *et al.* (Figure 28) exhibited histidine sensing capability in the presence of other amino acids.[103] The Buldurun group reported that Ru^{II} complex, 103 and Ni^{II} complex, 104 (Figure 43a) showed good enzyme inhibitions against carbonic anhydrase I and II isoenzymes (CA I and CA II) and acetylcholinesterase (AChE).[117]

3. Comparable Activities of Different Schiff-base Ligands and their Metallic Derivatives

In most cases, the metallic derivatives of Schiff-bases were found to exhibit higher activities than their parent ligands. The overall biological activities of Schiff-base ligands and their metallic derivatives have been summarized in Table 6. Neodymium (III) complexes 1 and 2 showed higher anti-microbial activities than those of their respective parent ligands L1 & L2. A maximum inhibition zones (IZ) of 86.5% and 88.3% were obained for 1 against Gram-positive bacterial speicies, *B. Subtilis* and fungal strain, *A. niger* at 100 μg mL^{-1}.[65] Co^{II} complex 13 were more active against Gram-positive bacteria compared to Gram-negative one with diameter of IZ: 45 mm for *B. Subtilis* (MIC_{50} values of >25 mg mL^{-1}) and 32 mm (MIC_{50} value of >50 mg mL^{-1}) for *P. vulgaris*.[70] The parent ligand L8 was less active than Co^{II} Complex 13. Similar selectivity was also observed for Ni^{II} complexes 14 and 15 which were the most effective against the Gram-positive bacteria, *S. aureus* (MTCC-740) with corresponding MIC values of 14 μg mL^{-1} and 18 μg mL^{-1}, respectively whereas against Gram-negative *E. coli* (MTCC-119), the MIC values for complexes 14 and 15 were 73 μg mL^{-1} and 77 μg mL^{-1}.[71] The complexes were also active against the fungal strains exhibiting the highest activities against *A. niger* (MTCC-281) and *C. tropicalis* (MTCC-230). Ni^{II} complex 17 showed higher anti-bacterial activity than its parent ligand L11 against *E. spp* with respective inhibition zone (IZ) values 40 mm & 24 mm.[72] Cu^{II} complexes 35,[83] 46–47[89] and Zn^{II} complex 49[90] showed remarkable anti-bacterial activity, whereas Zn^{II} complexes like 26, 27[76] and 43,[87] Ni^{II} complex 31,[81] and UO_2Saln complex 38[84] showed activity against both bacterial and fungal strains. Cu^{II} complex 35 (Figure 15) exhibited the highest activity against Gram-negative bacterial strain *E. coli* (MIC value of 1.25 mmol L^{-1}) which was actually higher than that of the reference drug Penicillin (MIC value of 10 mmol L^{-1}).[83] As usual, the parent ligand (L22) (MIC value of 5 mmol L^{-1} against *E. coli*) was less active than the complex. Cu^{II} complex 39, Co^{II} complex 40, Ni^{II} complex 41, Zn^{II} complex 42 and their parent ligand L24 acted differently against the fungal species *C. albicans* ($39 > 40 > 41 \geq 42 > L24$) (Figure 17).[86]

Several Schiff-base metal complexes exhibited promising anti-cancer activities.[61,73,75,76,99,100,102,104,107,111,112,115] (Table 6) Co^{II} complexes 52 and 56 showed activity against human small cell lung carcinoma A549 (IC_{50}: 65 μM & 50 μM),[61,99] Cu^{II} complexes 59 & 61 acted against lung carcinoma (H157) (IC_{50}: 1.54 ± 0.04 μM & 1.29 ± 0.06 μM),[100] 67 against Breast cancer cells (MDA-MB-231) (IC_{50}: 8.1 μM (72 h))[102] and 73 against cervical carcinoma cell line (HeLa) (IC_{50}: 11.02 ± 0.16 μM).[104] Zn^{II} complex 78 also showed remarkable activities against breast carcinoma MCF7 and prostate carcinoma DU145 (IC_{50}: 4.3 & 5.8 μM). The other complexes exhibiting significant anti-cancer activities included Ru^{II} complexes 82 & 92 (Lung carcinoma A549, IC_{50}: 2.37 ± 0.04 μM & 2.8 ± 1.0 μM respectively), Cd complex 99 (Colon cancer cell HT-29, IC_{50}: 2.57 ± 0.39 μg mL^{-1} (72 h)), La^{III} complex 100 (Colorectal adenocarcinoma cells (Caco-2), IC_{50}: 0.3772 μg mL^{-1}) and Ir^{III} complex 101 (Lung carcinoma A549, IC_{50}: 4.7 μM).

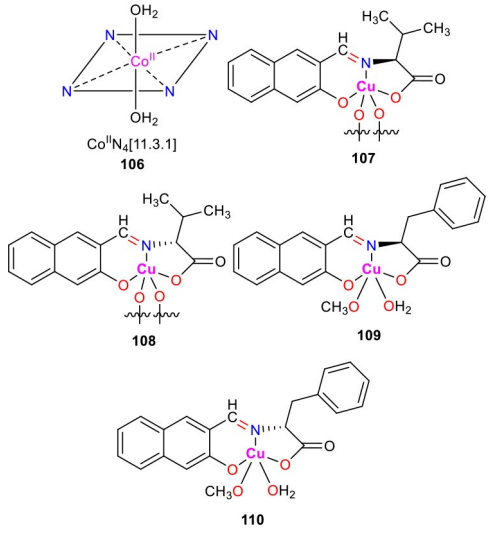

Figure 45. Structures of Co^{II} complex, **106**[125] and Cu^{II} complexes, **107–110**.[127]

4. Factors Affecting the Biological Properties

Different factors contribute significantly to the biological properties of the Schiff-basederivatives. The incorporation of metal ions into the Schiff-base ligands may render remarkable structural changes which, as a consequence, may affect the biological properties of the Schiff-base derivatives. In determining anti-bacterial behaviour of the metal complexes whereas chelation plays a significant role, several other important factors such as geometry of complexes, bond length between metal and the ligand, structural specificity, dipole moment, coordinating sites redox potential of metal ion, high toxicity of the metal complexes

Table 6. Different biological activities of Schiff-base ligands and their metallic derivatives.

Schiff-base Ligands/ Metal Complexes	Type of Activity	Pathogens/Target Cells/ Target compounds	Concentration (Conc.)/ IC_{50} Values	Inhibition Zone (IZ) Values	Minimum Inhibitory Concentration (MIC) Values	Ref.
Nd^{III} complex **1**	Anti-bacterial	*B. subtilis*	Conc. 100 μg mL^{-1}	86.5%	–	[65]
	Anti-fungal	*A. niger*	Conc. 100 μg mL^{-1}	88.3%	–	[65]
L1	Anti-bacterial	*B. subtilis*	Conc. 100 μg mL^{-1}	75.0%	–	[65]
	Anti-fungal	*A. niger*	Conc. 100 μg mL^{-1}	80.5%	–	[65]
Co^{II} Complex **13**	Anti-bacterial	*B. subtilis*	–	–	> 25 mg mL^{-1}	[70]
Ni^{II} complex **14**	Anti-bacterial	*S. aureus*	–	–	14 μg mL^{-1}	[71]
	Anti-fungal	*A. niger* (MTCC-281)	–	–	100 μg mL^{-1}	[71]
Ni^{II} complex **17**	Anti-bacterial	*E. sp*	–	40 mm	0.042 μmol mL^{-1}	[72]
L11	Anti-bacterial	*E. sp*	–	24 mm	–	[72]
Zn^{II} complex **26**	Anti-bacterial	*S. aureus*	–	–	0.0179 μM mL^{-1}	[76]
	Anti-fungal	*C. albicans*	–	–	0.0006 μM mL^{-1}	
Zn^{II} complex **27**	Anti-bacterial	*E. coli*	–	–	0.0160 μM mL^{-1}	[76]
	Anti-fungal	*A. niger*	–	–	0.0080 μM mL^{-1}	
Ni^{II} complex **31**	Anti-bacterial	*P. aeruginosa*	–	19 mm	–	[81]
	Anti-fungal	*C. albicans*	–	16 mm	–	
Cu^{II} complex **35**	Anti-bacterial	*E. coli*	–	–	1.25 mmol L^{-1}	[83]
L22	Anti-bacterial	*E. coli*	–	–	5 mmol L^{-1}	[83]
UO_2Saln Complex **38**	Anti-bacterial	*S. aureus*	Conc. 20 μg mL^{-1}	44 ± 0.25 mm	–	[84]
	Anti-fungal	*C. albicans*	Conc. 10 μg mL^{-1}	36 ± 0.17 mm	–	
L23	Anti-bacterial	*S. aureus*	Conc. 20 μg mL^{-1}	14 ± 0.24 mm	–	[84]
	Anti-fungal	*C. albicans*	Conc. 10 μg mL^{-1}	7 ± 0.16 mm	–	
Zn^{II} complex **43**	Anti-fungal	*C. Albicans, C. Tropicalis*	–	–	< 4.87 μg mL^{-1}	[87]
L25	Anti-fungal	*C. Albicans, C. Tropicalis*	–	–	78, 39 μg mL^{-1}	[87]
Cu^{II} complex **46**	Anti-bacterial	*E. coli, S. aureus*	–	–	64, 32 μg mL^{-1}	[89]
Cu^{II} complex **47**	Anti-bacterial	*E. coli, S. aureus*	–	–	64, 32 μg mL^{-1}	
Zn^{II} complex **49**	Anti-bacterial	*Bacillus SP*	–	–	50 mg mL^{-1}	[90]
Co^{II} complex **52**	Anti-cancer	A549 (human small cell lung carcinoma)	**IC_{50}**: 65 μM	–	–	[61]
Co^{III} complex **56**	Anti-cancer	A549 (human small cell lung carcinoma)	**IC_{50}**: 50 μM	–	–	[99]
Cu^{II} complex **59**	Anti-cancer	Lung carcinoma (H157)	**IC_{50}**: 1.54 ± 0.04 μM	–	–	[100]
L40	Anti-cancer	Lung carcinoma (H157)	**IC_{50}**: 2.32 ± 0.11 μM	-	–	[100]
Cu^{II} complex **61**	Anti-cancer	Lung carcinoma (H157)	**IC_{50}**: 1.29 ± 0.06 μM	–	–	[100]
Cu^{II} complex **67**	Anti-cancer	Breast cancer cells (MDA-MB-231)	**IC_{50}**: 8.1 μM (72 h)	–	–	[102]
Cu^{II} complex **73**	Anti-tumor	Cervical carcinoma cell line (HeLa)	**IC_{50}**: 11.02 ± 0.16 μM **IC_{50}**: 19.86 ± 0.62 μM	–	–	[104]
L49	Anti-tumor	Cervical carcinoma cell line (HeLa)		–		[104]
Zn^{II} complex **76**	Anti-tumor	Colon carcinoma HCT-116 cells	**IC_{50}**: 17.61 μg mL^{-1}	–	–	[73]
Zn^{II} complex **78**	Anti-cancer	Breast carcinoma MCF7	**IC_{50}**: 4.3 μM	–	–	[76]
		Prostate carcinoma DU145	**IC_{50}**: 5.8 μM	–	–	[76]
Ru^{II} complex **82**	Anti-proliferative	Lung carcinoma A549	**IC_{50}**: 2.37 ± 0.04 μM	–	-	[75]
	Anti-proliferative	Breast carcinoma MCF7	**IC_{50}**: 2.53 ± 0.10 μM	–	–	[75]
	Anti-oxidant	DPPH free radical	**IC_{50}**: 5.28 ± 0.24 μM	–	–	[75]
Ligand **L56**	Anti-oxidant	DPPH free radical	**IC_{50}**: 67.28 ± 1.44 μM	–	–	[75]
Ru^{II} complex **92**	Anti-tumor	Lung carcinoma A549	**IC_{50}**: 2.8 ± 1.0 μM	–	–	[107]
Cd^{II} complex **99**	Anti-cancer	Colon cancer cell HT-29	**IC_{50}**: 2.57 ± 0.39 μg mL^{-1} (72 h)	–	–	[111]
La^{III} complex **100**	Anti-cancer	Colorectal adenocarcinoma cells (Caco-2)	**IC_{50}**: 0.3772 μg mL^{-1}	–	–	[112]
L66	Anti-cancer	Colorectal adenocarcinoma cells (Caco-2)	**IC_{50}**: 0.4571 μg mL^{-1}	–	–	[112]
Ir^{III} complex **101**	Anti-cancer	Lung carcinoma A549	**IC_{50}**: 4.7 μM	–	–	[115]
Zn^{II} complex **33**	Anti-inflammatory	Bovine serum albumin (BSA)	Conc. 500 mg mL^{-1}	95.31 ± 3.1%	–	[82]
	Anti-inflammatory	Bovine serum albumin (BSA)				[124]
L20			Conc. 500 mg mL^{-1}	78.16 ± 2.0%	–	[82] [124]

at cell surface, solubility, steric, pharmacokinetic, concentration and hydrophobicity, can also influence substantially.[84] Sometimes, the ability of the central metal atom to increase its coordination number may also affect the anti-microbial property of the complexes and that's why, the metal atoms containing 4f orbitals exhibit relatively higher anti-microbial potential. The low lipid solubility of the complexes across the microbial walls, may result in the lower activity of complexes as compared to others.[85] In addition, the variation in the ribosomes of the various microbial cells or a difference in the cell membrane permeability of these microbes can lead to the variation in the activity of the metal complexes against the different microbes. Moreover, the electron-

withdrawing or electron-donating nature of the substituent groups present in Schiff-base metal complexes exert positive or negative influence on the anti-bacterial activities of the complexes.[69,76]

The presence of additional phenyl ring(s) in the Schiff-base ligand in the metal complexes affect the anti-microbial and anti-cancer activities of the complexes.[61,69] The higher DNA-binding propensity of the metal complexes result in higher anti-cancer activity which stem from the enhancement of stacking interaction of the metal complexes with the DNA bases due to the presence of additional phenyl groups in the complex moiety. Several metal complexes have been found to exhibit higher anti-cancer activities due to their higher degree of lipophilicity enabling them to bind with the receptor sites by crossing the lipid membrane.[100] In this regard, bromo-substituted compounds exhibit remarkable anti-cancer activity. The presence of a nitro group ($-NO_2$) in metal complexes results in remarkable cytotoxicity against the breast cancer cell lines due to their capability to generate selective intracellular reactive oxygen species (ROS) and the larger DNA fragmentation abilities in contact with the target cells.[102] The ability of the complexes to intercalate the DNA base pairs and/or their free radical scavenging activity may be the key point for some metal complexes to exhibit their anti-cancer activities.[75]

To this end, compounds can show efficient antioxidant activity by the effective radical scavenging ability which is facilitated through the proton (H) donating capabilities of the compounds.[116] The liberation of proton (H) by the metal complexes is facilitated by the presence of protonated functional group in the complex moiety. The radical-scavenging activity of the Schiff-base and its metal complexes may be enhanced through the presence of ample positive charge density in the central metal ions. Sometimes, the radical-scavenging activity of the Schiff-base and its metal complexes may also be affected by the presence of electron donor groups such as hydroxyl moiety in Schiff-base.[119]

5. Conclusions and Outlook

Schiff-base ligands possess exceptional structural flexibility and they can be modified into various metallic and non-metallic derivatives. Numerous articles on Schiff-bases and their metal complexes have been reported along with their interesting biological applications. The presence of nitrogen containing imine groups (–C=N–) in Schiff-bases give rise to their unique biological properties. On the other hand, the versatile biological applications of Schiff-base metal complexes stem from their increased lipophilicity resulting from the chelation of the Schiff-base ligands with the metal elements. The increased lipophilicity of the complexes improves their cell permeability which in turn allows them to exhibit better biological properties compared to the Schiff-base ligands themselves. The purpose of this Review article is to summarize various Schiff-base ligands and their different metal complexes reported in the last decade in a convenient way along with their important biological applications such as anti-bacterial and anti-fungal activities, anti-tumor and anti-cancer activities, anti-oxidant activities, anti-inflammatory activities and other therapeutic and medicinal activities. Development of new biologically active Schiff-bases and their metal complexes are now attracting the attention of medicinal chemists and pharmacists. The understanding of the structure-activity relationships of various Schiff-bases and their metallic derivatives mentioned in this Review article along with their mode of actions would guide the future researchers to identify new strategies for the development of new Schiff-bases and their different metallic derivatives with improved biological properties.

Acknowledgements

This work was supported by the Ministry of Science and Technoloy (MOST), Bangladesh. Dr. Bikash Dev Nath is thankful to BCSIR for a Postdoctotal Fellowship.

Conflict of Interest

The authors declare no conflict of interest.

Data Availability Statement

The data that support the findings of this study are available in the supplementary material of this article.

Keywords: Acyclic compounds · Biological activity · Metal complexes · Medicinal chemistry · Schiff-bases

[1] H. Schiff, *Justus Liebigs Ann. Chem.* **1864**, *131*, 118–119.
[2] Y. Xin, J. Yuan, *Polym. Chem.* **2012**, *3*, 3045–3055.
[3] Y. Jia, J. Li, *Chem. Rev.* **2015**, *115*, 1597–1621.
[4] M. Rezaeivala, H. Keypour, *Coord. Chem. Rev.* **2014**, *280*, 203–253.
[5] W. Qin, S. Long, M. Panunzio, S. Biondi, *Molecules.* **2013**, *18*, 12264–12289.
[6] C. M. da Silva, D. L. da Silva, L. V. Modolo, R. B. Alves, M. A. de Resende, C. V. B. Martins, *J. Adv. Res.* **2011**, *2*, 1–8.
[7] A. M. Abu-Dief, I. M. A. Mohamed, *J. Basic Appl. Sci.* **2015**, *4*, 119–133.
[8] K. Taguchi, F. H. Westheimer, *J. Org. Chem.* **1971**, *36*, 1570–1572.
[9] B. E. Love, J. Ren, *J. Org. Chem.* **1993**, *58*, 5556–5557.
[10] G. C. Look, M. M. Murphy, D. A. Campbell, M. A. Gallop, *Tetrahedron Lett.* **1995**, *36*, 2937–2940.
[11] A. K. Chakraborti, S. Bhagat, S. Rudrawar, *Tetrahedron Lett.* **2004**, *45*, 7641–7644.
[12] N. E. Borisova, M. D. Reshetova, Y. A. Ustynyuk, *Chem. Rev.* **2007**, *107*, 46–79.
[13] M. E. Belowicha, J. F. Stoddart, *Chem. Soc. Rev.* **2012**, *41*, 2003–2024.
[14] a) P. Przybylski, A. Huczynski, K. Pyta, B. Brzezinski, F. Bartl, *Curr. Org. Chem.* **2009**, *13*, 124–148; b) M. Pervaiz, S. Sadiq, A. Sadiq, U. Younas, A. Ashraf, Z. Saeed, M. Zuber, A. Adnan, *Coord. Chem. Rev.* **2021**, *447*, 214128.
[15] a) S. Omidi, A. Kakanejadifard, *RSC Adv.* **2020**, *10*, 30186–30202; b) H. Kargar, M. Fallah-Mehrjardi, R. Behjatmanesh-Ardakani, K. S. Munawar, M. Ashfaq, M. N. Tahir, *J. Mol. Struct.* **2021**, *1241*, 130653; c) P. Ghanghas, A. Choudhary, D. Kumar, K. Poonia, *Inorg. Chem. Commun.* **2021**, *130*, 108710.
[16] X. Tai, X. Yin, Q. Chen, M. Tan, *Molecules.* **2003**, *8*, 439–443.
[17] a) M. S. More, P. G. Joshi, Y. K. Mishra, P. K. Khanna, *Mater. Today Chem.* **2019**, *14*, 100195; b) W. A. Zoubi, Y. G. Ko, *J. Organomet. Chem.* **2016**, *822*, 173–188; c) M. E. Alkış, Ü. Keleştemür, Y. Alan, N. Turan, K. Buldurun, *J. Mol. Struct.* **2021**, *1226* 129402.
[18] M. A. Malik, O. A. Dar, P. Gull, M. Y. Wani, A. A. Hashmi , *MedChemComm* **2018**, *9*, 409–436.

[19] M. Ren, Z.-L. Xu, S.-S. Bao, T.-T. Wang, Z.-H. Zheng, R. A. S. Ferreira, L.-M. Zheng, L. D. Carlos, *Dalton Trans.* **2016**, *45*, 2974–2982.
[20] A. K. Asatkar, S. P. Senanayak, A. Bedi, S. Panda, K. S. Narayan, S. S. Zade, *Chem. Commun.* **2014**, *50*, 7036–7039.
[21] C. J. Whiteoak, G. Salassa, A. W. Kleij, *Chem. Soc. Rev.* **2012**, *41*, 622–631.
[22] P. Krishnamoorthy, P. Sathyadevi, R. R. Butorac, A. H. Cowley, N. S. P. Bhuvanesh, N. Dharmaraj, *Dalton Trans.* **2012**, *41*, 4423–4436.
[23] S. T. Chew, K. M. Lo, S. K. Sinniah, K. S. Sim, K. W. Tan, *RSC Adv.* **2014**, *4*, 61232–61247.
[24] F. Kitamura, K. Sawaguchi, A. Mori, S. Takagi, T. Suzuki, A. Kobayashi, M. Kato, K. Nakajima , *Inorg. Chem.* **2015**, *54*, 8436–8448.
[25] M. Bagherzadeh, M. Zare, *J. Coord. Chem.* **2012**, *65*, 4054–4066.
[26] R. Manikandan, P. Viswanathamurthi, M. Muthukumar, *Spectrochim. Acta A Mol. Biomol. Spectrosc.* **2011**, *83*, 297–303.
[27] P. Chellan, K. M. Land, A. Shokar, A. Au, S. H. An, C. M. Clavel, P. J. Dyson, C. de Kock, P. J. Smith, K. Chibale, G. S. Smith, *Organometallics.* **2012**, *31*, 5791–5799.
[28] W. Su, Q. Qian, P. Li, X. Lei, Q. Xiao, S. Huang, C. Huang, J. Cui, *Inorg. Chem.* **2013**, *52*, 12440–12449.
[29] T. Bal-Demirci, G. Congur, A. Erdem, S. Erdem-Kuruca, N. Ozdemir, K. Akgun-Dar, B. Varol, B. Ulkuseven, *New J. Chem.* **2015**, *39*, 5643–5653.
[30] M. Singh, S. K. Singh, M. Gangwar, G. Nath, S. K. Singh, *Med. Chem. Res.* **2016**, *25*, 263–282.
[31] R. Prabhakaran, P. Kalaivani, P. Poornima, F. Dallemer, G. Paramaguru, V. Vijaya Padma, R. Renganathan, R. Huang, K. Natarajan, *Dalton Trans.* **2012**, *41*, 9323–9336.
[32] R. Golbedaghi, A. M. Tabanez, S. Esmaeili, R. Fausto, *Appl. Organomet. Chem.* **2020**, *34*, e5884.
[33] N. E. Borisova, M. D. Reshetova, Y. A. Ustynyuk, *Chem. Rev.* **2007**, *107*, 46–79.
[34] R. Hernández-Molina, A. Mederos, *Comprehensive Coordination Chemistry II.* **2004**, *1*, 411–446.
[35] I. Ejidike, P. Ajibade, *Int. J. Mol. Sci.* **2016**, *17*, 60, and references cited therein.
[36] M. X. Li, C. L. Chen, D. Zhang, J. Y. Niu, B. S. Ji, *Eur. J. Med. Chem.* **2010**, *45*, 3169–3177.
[37] S. Parveen, *Appl. Organomet. Chem.* **2020**, *34*, e5687.
[38] W. A. Zoubia, A. A. S. Al-Hamdanib, M. Kaseem, *Appl. Organomet. Chem.* **2016**, *30*, 810–817.
[39] J. Magyari, B. B. Holló, L. S. Vojinović-Ješić, M. M. Radanović, S. Armaković, S. J. Armaković, J. Molnár, A. Kincses, M. Gajdács, G. Spengler, K. M. Szécsényi, *New J. Chem.* **2018**, *42*, 5834–5843.
[40] C. M. da Silva, D. L. da Silva, L. V. Modolo, R. B. Alves, M. A. de Resende, C. V. B. Martins, Â. De Fátima, *J. Adv. Res.* **2011**, *2*, 1–8.
[41] P. Przybylski, A. Huczynski, K. Pyta, B. Brzezinski, F. Bartl, *Curr. Org. Chem.* **2009**, *13*, 124–148.
[42] M. A. Hassan, A. M. Omer, E. Abbas, W. M. A. Baset, T. M. Tamer, *Sci. Rep.* **2018**, *8*, 1–14.
[43] A. M. Khan, O. u. R. Abid, S. Mir, *Biopolymers.* **2020**, *111*, e23338.
[44] P. S. Nayab, Akrema, I. A. Ansari, M. Shahid, Rahisuddin, *Luminescence.* **2017**, *32*, 829–838.
[45] J. R. Dilworth, R. Hueting, *Inorg. Chim. Acta* **2012**, *389*, 3–15.
[46] S. Patai, *Interscience, New York*, **1970**, pp. 149–180.
[47] A. Kajal, S. Bala, S. Kamboj, N. Sharma, V. Saini, *J. Catal.* **2013**, *893512*, 15.
[48] D. Chaturvedi, M. Kamboj, *Chem. Sci.* **2016**, *7*, e114/1–e114/2.
[49] K. N. Venugopala, B. S. Jayashree, *J. Heterocycl. Chem.* **2003**, *12*, 307–310.
[50] a) G. L. Eichhorn, I. M. Trachtenberg, *J. Am. Chem. Soc.* **1954**, *76*, 5183; b) G. L. Eichhorn, N. D. Marchand, *J. Am. Chem. Soc.* **1956**78, 2688; c) W. A. Zoubi, M. P. Kamil, S. Fatimah, N. Nashrah, Y. G. Ko, *Prog. Mater. Sci.* 2020, 112, 100663.
[51] a) G. B. Bagihalli, P. G. Avaji, S. A. Patil, P. S. Badami, *Eur. J. Med. Chem.* **2008**, *43*, 2639–2649; b) N. Dharamaraj, P. Viswanathamurthi, K. Natarajan, *Transition Met. Chem.* **2001**, *26*, 105–109; c) R. Malhota, S. Kumar, K. S. Dhindsa, *Indian J. Chem.* **1993**, *32 A*, 457–459.
[52] E. Canpolat, M. Kaya, *J. Coord. Chem.* **2004**, *57*, 1217.
[53] P. G. Cozzi, *Chem. Soc. Rev.* **2004**, *33*, 410.
[54] S. Ershad, L. Sagathforoush, G. Karim-Nezhad, S. Kangari, *Int. J. Electrochem. Sci.* **2009**, *4*, 846–854.
[55] M. L. Low, L. Maigre, P. Dorlet, R. Guillot, J.-M. Pagès, K. A. Crouse, C. Policar, N. Delsuc, *Bioconjugate Chem.* **2014**, *25*, 2269–2284.
[56] M. J. Chow, C. Licona, D. Yuan Qiang Wong, G. Pastorin, C. Gaiddon, W. H. Ang, *J. Med. Chem.* **2014**, *57*, 6043–6059.
[57] S. Savir, Z. J. Wei, J. W. K. Liew, I. Vythilingam, Y. A. L. Lim, H. M. Saad, K. S. Sim, K. W. Tan, *J. Mol. Struct.* **2020**, *1211*, 128090.
[58] A. Biswas, L. K. Das, M. G. B. Drew, G. Aromí, P. Gamez, A. Ghosh, *Inorg. Chem.* **2012**, *51*, 7993–8001.
[59] N. Kushwah, M. K. Pal, A. Wadawale, V. Sudarsan, D. Manna, T. K. Ghanty, V. K. Jain, *Organometallics.* **2012**, *31*, 3836–3843.
[60] S. M. Wilkinson, T. M. Sheedy, E. J. New, *J. Chem. Educ.* **2016**, *93*, 351–354.
[61] S. Ambika, Y Manojkumar, S. Arunachalam, B. Gowdhami, K. K. M. Sundaram, R. V. Solomon, P. Venuvanalingam, M. A. Akbarsha, M. Sundararaman, *Sci. Rep.* **2019**, *9*, 1–14.
[62] F. Han, Q. Teng, Y. Zhang, Y. Wang, Q. Shen, *Inorg. Chem.* **2011**, *50*, 2634–2643.
[63] A. Hussain, M. F. AlAjmi, M. T. Rehman, S. Amir, F. M. Husain, A. Alsalme, M. A. Siddiqui, A. A. AlKhedhairy, R. A. Khan, *Sci. Rep.* **2019**, *9*, 1–17.
[64] R. M. El-Ferjani, M. Ahmad, S. M. Dhiyaaldeen, F. W. Harun, M. Y. Ibrahim, H. Adam, B. M. Yamin, M. M. J. Al-Obaidi, R. A. Batran, *Sci. Rep.* **2016**, *6*, 38748.
[65] Q. Ain, S. K. Pandey, O. P. Pandey, S. K. Sengupta, *Appl. Organomet. Chem.* **2016**, *30*, 102–108.
[66] W. H. Mahmoud, R. G. Deghadi, G. G. Mohamed, *Appl. Organomet. Chem.* **2016**, *30*, 221–230.
[67] S. Y. Ebrahimipoura, I. Sheikhshoaiea, J. Castro, M. Dušek, Z. Tohidian, V. Eigner, M. Khaleghi, *RSC Adv.* **2015**, *5*, 95104–95117.
[68] D. Biswal, N. R. Pramanik, S. Chakrabarti, N. Chakraborty, K. Acharya, S. S. Mandal, S. Ghosh, M. G. B. Drew, T. K. Mondal, S. Biswas, *New J. Chem.* **2015**, *39*, 8681–8694.
[69] P. Bhatra, J. Sharma, R. A. Sharma, Y. Singh, *Appl. Organomet. Chem.* **2017**, *31*, 8pp.
[70] E. M. Zayed, A. M. M. Hindy, G. G. Mohamed, *Appl. Organomet. Chem.* **2018**, *32*, e4603.
[71] P. Raj, A. Singh, A. Singh, N. Singh, *ACS Sustainable Chem. Eng.* **2017**, *5*, 6070–6080.
[72] J. R. Anacona, K. Ruiz, M. Loroño, F. Celis, *Appl. Organomet. Chem.* **2019**, *33*, e4744.
[73] A. S. Alturiqi, A. N. M. A. Alaghaz, M. E. Zayed, R. A. Ammar, *J. Chin. Chem. Soc.* **2018**, *65*, 1060–1074.
[74] I. Ameen, A. K. Tripathi, R. L. Mishra, A. Siddiqui, U. N. Tripathi, *RSC Adv.* **2018**, *8*, 8412–8425.
[75] G. Kalaiarasi, S. R. J. Rajkumar, S. Dharani, J. G. Małeckic, R. Prabhakaran, *RSC Adv.* **2018**, *8*, 1539–1561.
[76] J. Devi, M. Yadav, D. Kumar, L. S. Naik, D. K. Jindal, *Appl. Organomet. Chem.* **2019**, *33*, e4693.
[77] M. S. Kasare, P. P. Dhavan, B. L. Jadhav, S. D. Pawar, *ChemistrySelect* **2019**, *4*, 10792–10797.
[78] P. Jain, D. Kumar, S. Chandra, N. Misra, *Appl. Organomet. Chem.* **2020**, *34*, e5371.
[79] W. A. Zoubi, V. Y. Jirjees, V. T. Suleman, A. A. S. Al-Hamdani, S. D. Ahmed, Y. G. Kim, Y. G. Ko, *J. Phys. Org. Chem.* **2019**, *32(11)*, e4004.
[80] K. Peewasan, M. P. Merkel, K. Zarschler, H. Stephan, C. E. Anson, A. K. Powell, *RSC Adv.* **2019**, *9*, 24087–24091.
[81] A. Z. El-Sonbati, W. H. Mahmoud, G. G. Mohamed, M. A. Diab, S. M. Morgan, S. Y. Abbas, *Appl. Organomet. Chem.* **2019**, *33*, e5048.
[82] M. Murugaiyan, S. P. Manib, M. A. Sithique, *New J. Chem.* **2019**, *43*, 9540–9554.
[83] Y. Guo, X. Hu, X. Zhang, X. Pu, Y. Wang, *RSC Adv.* **2019**, *9*, 41737–41744.
[84] M. S. S. Adam, O. M. El-Hadyb, F. Ullah, *RSC Adv.* **2019**, 9, 34311–34329.
[85] J. Devi1, M. Yadav, D. K. Jindal, D. Kumar, Y. Poornachandra, *Appl. Organomet. Chem.* **2019**, *33*, e5154.
[86] O. A. Dar, S. A. Lone, M. A. Malik, M. Y. Wani, A. Ahmad, A. A. Hashmi, *RSC Adv.* **2019**, *9*, 15151–15157.
[87] E. Alterhoni, A. Tavman, D. Gürbüz, M. Hacioglu, A. Çinarli, O. Şahin, A. S. B. Tan, *ChemistrySelect* **2020**, *5*, 9730–9735.
[88] T. Chowdhury, S. Dasgupta, S. Khatua, K. Acharya, D. Das, *ACS Appl. Bio Mater.* **2020**, *3*, 4348–4357.
[89] a) H. Kargar, F. Aghaei-Meybodi, R. Behjatmanesh-Ardakani, M. R. Elahifard, V. Torabi, M. Fallah-Mehrjardi, M. N. Tahir, M. Ashfaq, K. S.

Munawar, *J. Mol. Struct.* **2021**, 1230, 129908; b) H. Kargar, F. Aghaei-Meybodi, M. R. Elahifard, M. N. Tahir, M. Ashfaq, K. S. Munawar, *J. Coord. Chem.* **2021**, *74*, 1534–1549.
[90] S. Mahato, N. Meheta, M. Kotakonda, M. Joshi, M. Shit, A. R. Choudhury, B. Biswas, *Polyhedron.* **2021**, *194*, 114933.
[91] D. O. Maia, V. F. Santos, C. R. S. Barbosa, Y. N. Fróes, D. F. Muniz, A. L. E. Santos, M. H. C. Santos, R. R. S. Silva, C. G. L. Silva, R. O. S. Souza, J. C. S. Sousa, H. D. M. Coutinho, C. S. Teixeira, *Chem.-Biol. Interact.* **2022**, *351*, 109714.
[92] S. Dilruba, G. V. Kalayda, *Cancer Chemother. Pharmacol.* **2016**, *77*, 1103–1124.
[93] G. Giaccone, R. S. Herbst, G. Giaccone, J. H. Schiller, R. B. Natale, V. Miller, C. Manegold, G. Scagliotti, R. Rosell, I. Oliff, J. A. Reeves, M. K. Wolf, A. D. Krebs, S. D. Averbuch, J. S. Ochs, J. Grous, A. Fandi, D. H. Johnson *J. Clin. Oncol.* **2004**, *22*, 777–784.
[94] L. Zeng, Y. Chen, J. Liu, H. Huang, R. Guan, L. Ji, H. Chao, *Sci. Rep.* **2016**, *6*, 19449.
[95] F.-X. Wang, M.-H. Chen, X.-Y. Hu, R.-R. Ye, C.-P. Tan, L.-N. Ji, Z.-W. Mao, *Sci. Rep.* **2016**, *6*, 38954.
[96] R. A. Khan, M. Usman, R. Dhivya, P. Balaji, A. Alsalme, H. AlLohedan, F. Arjmand, K. AlFarhan, M. A. Akbarsha, F. Marchetti, C. Pettinari, S. Tabassum, *Sci. Rep.* **2017**, *7*, 45229.
[97] J.-L. Qin, W.-Y. Shen, Z.-F. Chen, L.-F. Zhao, Q.-P. Qin, Y.-C. Yu, H. Liang, *Sci. Rep.* **2017**, *7*, 46056.
[98] A. P. King, H. A. Gellineau, J.-E. Ahn, S. N. MacMillan, J. J. Wilson, *Inorg. Chem.* **2017**, *56*, 6609–6623.
[99] A. P. King, H. A. Gellineau, S. N. MacMillan, J. J. Wilson, *Dalton Trans.* **2019**, *48*, 5987–6002.
[100] H. Pervez, M. Ahmad, S. Zaib, M. Yaqub, M. M. Naseer, J. Iqbal, *MedChemComm* **2016**, *7*, 914–923.
[101] C. Elamathi, R. Butcher, R. Prabhakaran, *Appl. Organomet. Chem.* **2019**, *33*, e4659.
[102] L. Rigamonti, F. Reginato, E. Ferrari, L. Pigani, L. Gigli, N. Demitri, P. Kopel, B. Tesarovad, Z. Heger, *Dalton Trans.* **2020**, *49*, 14626–14639.
[103] A. Mondal, C. Das, M. Corbella, A. Bauzá, A. Frontera, M. Saha, S. Mondal, K. D. Sahad, S. K. Chattopadhyay, *New J. Chem.* **2020**, *44*, 7319–7328.
[104] C. Balakrishnan, S. Natarajan, M. A. Neelakantan, *RSC Adv.* **2016**, *6*, 102482–102497.
[105] R. M. Ramadan, W. M. Elsheemy, N. S. Hassan, A. A. A. Aziz, *Appl. Organomet. Chem.* **2018**, *32*, e4180.
[106] M. J. Chow, M. V. Babak, D. Y. Q. Wong, G. Pastorin, C. Gaiddon, W. H. Ang, *Mol. Pharm.* **2016**, *13*, 2543–2554.
[107] S. Chen, X. Liu, J. Huang, X. Ge, Q. Wang, M. Yao, Y. Shao, T. Liu, X–A. Yuan, L. Tiana, Z. Liu, *Dalton Trans.* **2020**, *49*, 8774–8784.
[108] V. P. Petrović, M. N. Živanović, D. Simijonović, J. Đorović, Z. D. Petrović, S. D. Marković, *RSC Adv.* **2015**, *5*, 86274–86281.
[109] G. Kalaiarasi, G. Aswini, S. R. J. Rajkumar, S. Dharani, V. M. Lynch, R. Prabhakaran, *Appl. Organomet. Chem.* **2018**, *32*, e4466.
[110] S. N. Mbugua, N. R. S. Sibuyi, L. W. Njenga, R. A. Odhiambo, S. O. Wandiga, M. Meyer, R. A. Lalancette, M. O. Onani, *ACS Omega.* **2020**, *5*, 14942–14954.
[111] M. Hajrezaie, M. Paydar, C. Y. Looi, S. Z. Moghadamtousi, P. Hassandarvish, M. S. Salga, H. Karimian, K. Shams, M. Zahedifard, N. A. Majid, H. M. Ali, M. A. Abdulla, *Sci. Rep.* **2015**, *5*, 9097.
[112] H. M. Aly, R. H. Taha, N. M. El-deeb, A. Alshehri, *Inorg. Chem. Front.* **2018**, *5*, 454–473.
[113] I. P. Ejidike, P. A. Ajibade, *Rev. Inorg. Chem.* **2015**, *35*, 191–224.
[114] S. Yadamani, A. Neamati, M. Homayouni-Tabrizi, S. A. Beyramabadi, S. Yadamani, A. Gharib, A. Morsali, M. Khashi, The *Breast.* **2018**, *41*, 107–112.
[115] Y. Yang, L. Guo, Z. Tian, X. Ge, Y. Gong, H. Zheng, S. Shi, Z. Liu, *Organometallics.* **2019**, *38*, 1761–1769.
[116] R. Amorati, M. Lucarini, V. Mugnaini, G. F. Pedulli, *J. Org. Chem.* **2003**, *68*, 5198–5204.
[117] K. Buldurun, N. Turan, A. Aras, A. Mantarcı, F. Turkan, E. Bursal, *Chem. Biodiversity* **2019**, *16*, e1900243.
[118] S. M. Emam, S. A. Abouel-Enein, E. M. Abdel-Satar, *Appl. Organomet. Chem.* **2019**, *33*, e4847.
[119] W. A. Zoubi1, M. J. Kim, A. A. S. Al-Hamdani, Y. G. Kim, Y. G. Ko, *Appl. Organomet. Chem.* **2019**, *33*, e5210.
[120] E. Siegmund, R. Cadmus, G. A. Lu, *Proc. Soc. Exp. Biol. Med.* **1957**, *95*, 729–731.
[121] J. J. Loux, P. D. DePalma, S. L. Yankell, *Toxicol. Appl. Pharmacol.* **1972**, *22*, 672–675.
[122] C. A. Winter, E. A. Risley, G. W. Nuss, *Proc. Soc. Exp. Biol. Med.* **1962**, *111*, 544–547.
[123] R. Koster, M. Anderson, D. E. J. Beer, *Proc. Soc. Exp. Biol. Med.* **1959**, *18*, 412–415.
[124] R. Sribalan, M. Kirubavathi, G. Banuppriya, V. Padmini, *Bioorg. Med. Chem. Lett.* **2015**, *25*, 4282–4286.
[125] H. Praekunatham, K. K. Garrett, Y. Bae, A. A. Cronican, K. L. Frawley, L. L. Pearce, J. Peterson, *Chem. Res. Toxicol.* **2020**, *33*, 333–342.
[126] J. E. Baumeister, K. M. Reinig, C. L. Barnes, S. P. Kelley, S. S. Jurisson, *Inorg. Chem.* **2018**, *57*, 12920–12933.
[127] S. Zehra, T. Roisnel, F. Arjmand, *ACS Omega.* **2019**, *4*, 7691–7705.

Submitted: December 2, 2021
Accepted: March 16, 2022